

THESIS

Kiflu Hiyabu Jimie
MSc. Environmental Engineering

Gödöllő
2023



**Hungarian University of Agriculture and Life Science
Szent István Campus
MSc. Environmental Engineering**

**ANALYSIS OF SURFACE WATER WITH SPECTRAL
PROPERTIES OF LIGHT**

Primary Supervisor: Dr. András Barczy
Assistant Professor

Author: Kiflu Hiyabu Jimie
F78NTE

Institute/Department: Institute of Environmental Sciences

**Gödöllő
2023**

Table of Contents

| | |
|--|----|
| List of Figures..... | 3 |
| List of Tables..... | 3 |
| Abbreviations and Notations..... | 4 |
| 1. INTRODUCTION..... | 5 |
| 1.1 Background..... | 5 |
| 1.2 Objectives..... | 7 |
| 2. LITERATURE REVIEW..... | 8 |
| 2.1 Electromagnetic Radiation and Light..... | 8 |
| 2.1.1 Interaction of Light with Matter..... | 9 |
| 2.1.2 Luminous Intensity and Candela..... | 9 |
| 2.2 Light Distribution and Colour Dimensions..... | 10 |
| 2.2.1 Colour Measurement..... | 10 |
| 2.2.2 Human Perception..... | 10 |
| 2.2.3 Colorimetry and CIE System..... | 11 |
| 2.2.4 Color Models..... | 11 |
| 2.2.4.1 RGB Color Model..... | 11 |
| 2.2.4.2 CIELAB Colour Model..... | 12 |
| 2.2.4.3 CIE 1931-XYZ Color Model | 13 |
| 2.2.4.4 CMYK Color Model..... | 14 |
| 2.2.4.5 HSV Color Model..... | 15 |
| 2.2.5 Digital Color and Computer Vision..... | 16 |
| 2.2.5.1 Image Capture and Processing..... | 16 |
| 2.3 Water Quality Parameters..... | 17 |
| 2.3.1 Water Quality..... | 17 |
| 2.3.2 Nitrate..... | 17 |
| 2.3.3 Phosphate..... | 19 |
| 2.3.4 Source of Nitrate and Phosphate..... | 20 |
| 2.3.4.1 Agricultural Activity..... | 20 |
| 2.3.4.2 Urban Activity..... | 20 |
| 2.3.4.3 Land Use Change..... | 21 |
| 2.4 Water Quality Measurement..... | 21 |
| 2.4.1 Analytical Techniques..... | 21 |
| 2.4.1.1 Colorimetric Technique..... | 22 |
| 2.4.1.2 Ultraviolet-Visible Technology..... | 22 |
| 2.4.1.6 Fluorescence technique..... | 23 |
| 2.4.2 Remote Sensing Technology..... | 24 |
| 2.4.2.1 Satellite Water Quality Detection..... | 24 |
| 2.4.2.3 Aircraft Water Quality Detection..... | 27 |
| 2.4.2.4 Smartphone Water Quality Detection..... | 28 |
| 3. MATERIAL AND METHOD..... | 31 |
| 3.1. Research site..... | 31 |
| 3.2 Methods and Measurement..... | 32 |
| 3.2.1 eXact iDip Photometer..... | 32 |
| 3.2.2 Photometric test procedures..... | 33 |
| 3.2.3 Sample Collection for Analytical Analysis..... | 34 |
| 3.2.4 Image Acquisition..... | 34 |

| | |
|---|----|
| 3.2.3 Nix Quality Control Sensor..... | 35 |
| 3.2.3.1 Toolkit Smartphone Application..... | 36 |
| 3.2.3.2 Nix Quality Control Sensor and Data collection..... | 36 |
| 3.2.4 Color Analyser Smartphone Application..... | 37 |
| 3.3.5 Statistical Data Analysis..... | 38 |
| 4. RESULT AND EVALUATION..... | 40 |
| 4.1 Photometric Results Analysis..... | 40 |
| 4.2 Nix Quality Control Result Analysis..... | 42 |
| 4.3 Smartphone camera image analysis..... | 46 |
| 4.4 Nix QC and Smartphone Results Comparison..... | 50 |
| 5. CONCLUSION AND RECOMMENDATION..... | 53 |
| 6. SUMMARY..... | 55 |
| 7. ACKNOWLEDGEMENT..... | 56 |
| 8. REFERENCES..... | 57 |
| 9. APPENDIX..... | 65 |
| 10. DECLARATION..... | 68 |

List of Figures

| | |
|---|----|
| Figure 1. The Electromagnetic Spectrum | 8 |
| Figure 2. Plane-polarized Electromagnetic Radiation, Consisting of a Single Oscillating Electric Field Oscillating Magnetic Field | 9 |
| Figure 3. 3-Dimensional RGB Color Distribution..... | 12 |
| Figure 4. CIELAB 1976 Color Sphere..... | 13 |
| Figure 5. CIE XYZ 1931 Color Space..... | 14 |
| Figure 6. Schematic Diagram among the a RGB, b CMYK, c HSV, and d CIELAB Color Models..... | 15 |
| Figure 7. Bayer Filter Array and its Positioning on the Photodetector Array of Image Process..... | 16 |
| Figure 8. Image of Study Area (Gödöllő Állami-telepek) | 31 |
| Figure 9. Three-Dimensional Image of the Study Area..... | 32 |
| Figure 10. eXact iDip Smart Photometer..... | 32 |
| Figure 11. eXact iDip Smart Digital Photometer Testing Steps..... | 33 |
| Figure 12. Parts of Nix QC Color Sensor..... | 35 |
| Figure 13. Nix QC Sensor and Toolkit Mobile Application..... | 37 |
| Figure 14. RGB Color Analyser Smartphone Application..... | 37 |
| Figure 15. Nitrate and Phosphate Concentration Graph..... | 41 |
| Figure 16. Correlation between Nitrate and Phosphate..... | 41 |
| Figure 17. Nix Quality Control Sensor RGB Color Vales Scatter Graph | 43 |
| Figure 18. Power Relation Between Nitrate, Phosphate Concentrations and Nix QC RGB Color Values..... | 44 |
| Figure 19. Nitrate Concentration and NIX QC Blue Color Validation Model..... | 45 |
| Figure 20. Phosphate Concentration and NIX QC Green Color Validation Model..... | 45 |
| Figure 21. Smartphone Camera RGB Color Value Scatter Graph..... | 47 |
| Figure 22. Power Relation between Nitrate, Phosphate Concentrations and Smartphone Camera RGB Color Values..... | 48 |
| Figure 23. Nitrate Concentration and Smartphone Blue Color Validation Model..... | 49 |
| Figure 24. Phosphate Concentration and Smartphone Green Color Validation Model..... | 49 |
| Figure 25. Nix QC and Smartphone CIELAB Lightness Comparsion Graph..... | 50 |
| Figure 26. CIELAB Lightness Scatter Plot between Nix QC and Smartphone | 51 |
| Figure 27. Correlation between Nix QC and Smartphone CIELAB Lightness..... | 52 |
| Figure 28. Nix QC and Smartphone Regression Model Analysis..... | 52 |

List of Tables

| | |
|--|----|
| Table 1. Descriptive statistics of water quality variables for 31 water samples collected from study area..... | 40 |
| Table 2. Statistical analysis for RGB color values obtained from NIX QC sensor..... | 42 |
| Table 3. Statistical analysis for RGB color results obtained Smartphone camera..... | 46 |

Abbreviations and Notations

| Symbol | Definition |
|-----------------|--|
| RGB | Red, Green, Blue |
| CO | Coefficient of Variance |
| SDV | Standard Deviation |
| DN _s | Digital Numbers |
| CMOS | Complementary Metal Oxide Semiconductors |
| NIX QC | Nix Quality Control sensors |
| Min | Minimum |
| Max | Maximum, |
| AVG | Average |
| GQM_ | Goal Question Metric |
| EOW | EyeOnWater |
| UAS | Unmanned Aircraft System |
| AVIRIS-NG | Airborne Visible/Infrared Imaging Spectrometer New Generation |
| ETM | Enhanced Thematic Mapper |
| GOCI | Geostationary Ocean Color Imager |
| LISS | Linear Imaging Self-Scanning Sensor |
| TSI | Trophic Status Index |
| _FUI | Forel-Ule Index |
| CDOM | Colored Dissolved Organic Matter |
| GA-PLS | Genetic Algorithms and Partial Least Squares |
| MODIS | Moderate Resolution Imaging Spectroradiometer |
| MERIS | Medium Resolution Imaging Spectrometer |
| TM | Thematic Mapper |
| RS | Remote sensing |
| NIR | Near Infrared |
| UV | Ultraviolet |
| EPA | Environmental Protection Agency |
| WHO | World Health Organization |
| CIE | International Commission on Illumination |
| SI | International System |
| cd | candela |
| LAB | Lightness, A=Red and Green, B=Blue and Yellow |
| APP | Application |

1. INTRODUCTION

1.1 Background

Water is an absolutely essential segment of the ecosystem, which is an indispensable factor of existence, and it helps modulate the temperature of the environment (Chaplin, 2001). They are of overriding value in lengthening all forms of life. Moreover, water helps preserve the variety of life in wetland ecosystems by providing habitats to a superfluity of living organisms (Xie et al., 2018). It is not only critical to ecosystems as a keystone component of the hydrologic cycle but also touches every aspect of our lives, such as drinking water, agriculture, electricity production, recreation, fishing, transportation, and industrial purposes (Reddy et al., 2021).

Around the world today, environmental irregularity is seen as the main issue, as a result of human pressure on environment (Schwarzenbach et al., 2010). Due to the fast increase in human population along coastal areas and riverbanks, the habitats of fish and other aquatic species may be negatively impacted by any changes made to these delicate ecosystems as a result of human-induced nutrient pollution. Human activities, including intensive farming and domestic and livestock wastewater discharge, can lead to a rise in the nitrate and phosphate levels in nearby waters, cause the water to fall asleep, and cause algal proliferation that negatively impacts water clarity, food sources, and habitats (Qin, 2009).

Nitrate and phosphate are two major nutrients required by living things for their physiological functions. However, if their concentration exceeds the advised limit, they are regarded as pollutants. In addition, surface water with high nutrient loads (nitrate and phosphate) encourage the growth of water plants but has a negative impact on water quality by promoting the establishment of algal bloom and foul odours (Mènesguen et al., 2018). This results in a significant loss of dissolved oxygen in the surface water. The amount of dissolved oxygen in the surface water decreases dramatically, causing suffocation and the death of aquatic plants and animals (Yalç et al., 2017; Yona et al., 2023).

Abnormal increases in nitrate effluent in potable water are also associated with several disorders of body function, such as breast cancer risk and thyroid diseases in humans (Ward et al., 2018). Besides, high phosphate levels have been linked to several clinical outcomes, including hypophosphatemia, which raises the risk of cardio-metabolic illnesses. Furthermore,

excessive phosphate has been implicated in some renal diseases, and long-term exposure to high-concentration phosphate-containing safe water has been responsible for causing damage to human accessory organs of digestive system (Mironov et al., 2022).

A sturdy ecosystem is typically indicated by clean water sources. Thus, water quality sensing with advanced technology is an integral part of taking care of the environment. The requirement for sustainable surface water necessitates ongoing assessments of the quality of currently available water supplies and associated watersheds under more precise control and management strategies. Likewise, the level of treatment required for human consumption, agribusiness, and factory operations demands an understanding of the quality of water fountains (Bhateria & Jain, 2016).

Indicators of surface water quality, such as nitrate and phosphate parameters, are typically found by gathering samples in the field and analysing them in a lab. Since this ex-situ assessment requires hard work and time-consuming procedures, it is not suited for field-based autonomous operation, despite the fact that it gives excellent precision (Das et al., 2022; Juncal et al., 2020). Additionally, traditional point sample techniques struggle to detect the geographical or temporal fluctuations in water quality that are essential for thorough evaluation and management of surface water, and it is not possible to produce a simultaneous water quality database on a regional scale.

Conventional methods of quantitative surface water analysis use professional and high-priced technology with highly skilled personnel to dissect samples taken from the field and sent to laboratories. Hence, environmental monitoring has gradually entered the realm of multi-source mass data. The use of traditional observational and satellite remote detection information for water quality monitoring is no longer sufficient due to the rapid development of contemporary huge data technology and the communication profession, as well as growing citizen interest in environmental quality. In this regard, intelligent digital devices show great potential, providing new possibilities for water quality sensing (Gao et al., 2022).

The colour of surface water has long been a reliable qualitative indicator of the water's quality. Hence, color models were developed for quantitative water quality variable measurement. A colour is measured as an amount of radiation reflected or transmitted from a colour stimulus over the specified wavelength range. Color conveys spectral information in

the form of large regions in the red, green, and blue portions of the visible spectrum. Using the amount of light measured by the detector, the red, green, and blue (RGB) values were assigned to each pixel. Thus, the RGB values detected by digital imaging technology helps for water quality monitoring (Goddijn & White, 2006).

Hand-held digital cameras and smartphone cameras have high surface resolution and time flexibility and are not affected by cloudy conditions. Thus, they can complement satellite remote detection technology, which is affected by cloud concealment (Abdelmalik, 2018). However, how to make effective quantitative use of the citizen science data acquired from the handheld cameras and incorporate it into scientific research is a difficult issue to tackle. Due to their greater photography features, software, and portability for image processing, smartphones are the best image capture equipment (Abughrin et al., 2022).

1.2 Objectives

The primary goal of this study was to strengthen the monitoring, evaluation, and governance of surface water quality and to find out how communities react to smartphone water quality assessment applications in terms of their efficacy, usefulness, and contentment compared to conventional instruments. Besides, this work focuses on how digital pictures taken on smartphones are used for the investigation of water quality, including the fundamentals of the technology, the tools used to capture images, the color spaces used, and the handling of research analysis. Moreover, it is a thesis aims to overcome the challenges of successive and integrated sampling, which turn into a major barrier to the management and monitoring of water quality.

2. LITERATURE REVIEW

2.1 Electromagnetic Radiation and Light

Our daily lives depend on light, which also improves our living conditions and is a crucial component of optics, solar energy, and modern lighting technologies. Moreover, electromagnetic radiation, which includes not only the ultraviolet, visible, and infrared regions but additionally the X-ray, gamma-ray, and radio ranges, can also be referred to as "light" in some contexts (Figure 1.). Depending on the situation, light can have a wide variety of meanings. It is described as electromagnetic radiation, which used to represent the ultraviolet, visible, and infrared portions of the electromagnetic spectrum in the sense that they generally characterized optical radiation. It is a property of all feelings and recognition that is unique to vision when it is used to express a light stimulus, and it is radiation that is taken into consideration from the point of view of its capacity to activate the visual system in humans (Gardi, 2018).

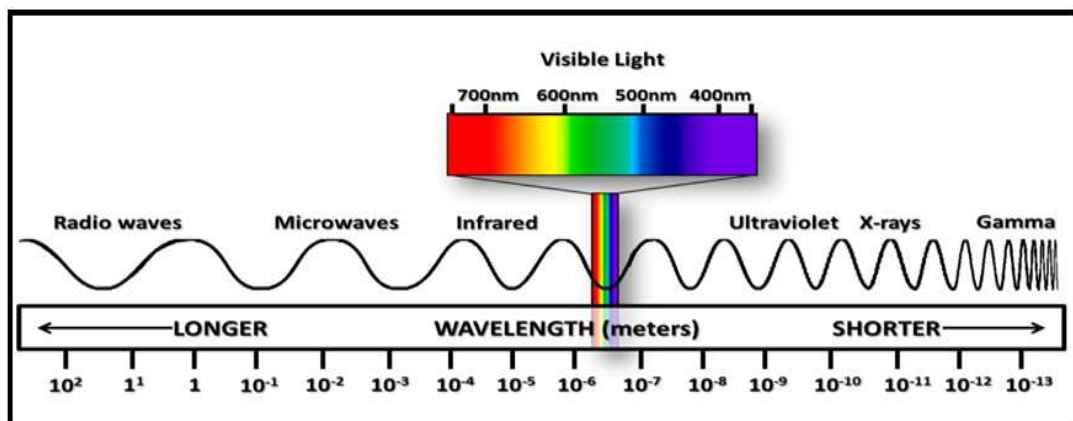


Figure 1. The Electromagnetic Spectrum. Source: (*Web 1*, n.d.)

The release or transmission of energy in the form of electromagnetic waves and photons is known as electromagnetic radiation. Another way to define electromagnetic radiation is as the emission or transfer of energy from vibrating charged particles that results in a disturbance in the form of oscillating electric and magnetic fields. The term electromagnetic waves was coined because electric and magnetic waves constantly coexisted or were linked. Also, it was discovered that the lines of force for these electric and magnetic waves were always parallel to one another and parallel to the direction in which the waves were propagating (Figure 2.).

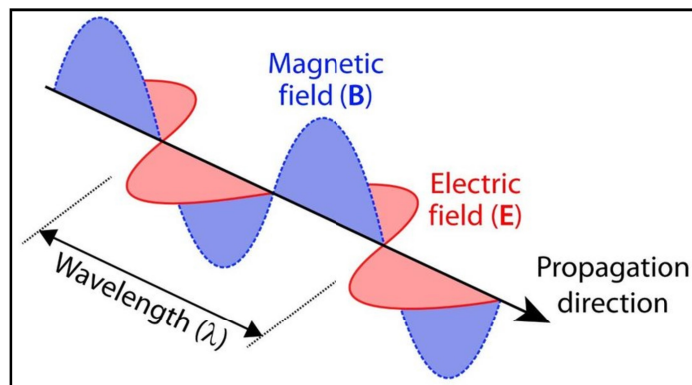


Figure 2. Plane-polarized Electromagnetic Radiation, Consisting of a Single Oscillating Electric Field and Magnetic Field.(Verhoeven, 2017)

2.1.1 Interaction of Light with Matter

In accordance with the connection between the light's wavelength and the intervening matter's overall size, many miracles can emerge when the light gets in contact with material. The visual detectors in the naked eye can be stimulated by visible light from the spectrum. Light dispersion and interruption work together to create a wide range of colors. For example, Rayleigh scattering occurs when light waves meet with small interfering particles, such as when visible light interacts with airborne dust or gas molecules, giving the sky its blue color. Moreover, when visible light interacts with large molecules like clouds in the atmosphere, Mie scattering appear which produce the white color of clouds. However, when light interacts with objects that are large in relation to their wavelength (Crowell, 2000).

The light will either be reflected, refracted, transmitted, absorbed, or scattered based on the transparency of the substance and the nature of its surface. The exact nature of the substance will determine the dominant kind of light engagement; for example, a polished, opaque, colorless solid will exhibit specular reflection, but an opaque, colorful substance will exhibit diffuse reflection or scattering. The unevenly reflecting material selectively alters the incident light's energy distribution, producing various hues as a result.

2.1.2 Luminous Intensity and Candela

According to the luminosity function, a conventional description of the sensitivity of the visual system, luminous intensity in photometry is a measurement of the wave length-

weighted energy that a light source emits in a given direction per unit solid angle. The candela (cd), a SI unit, represents light intensity. The measuring of visible light as seen by naked eyes is referred to as photometry. The human eye can only perceive the visible portion of the spectrum, and it responds differently to light of various spectrum wavelengths. Other wavelengths of light that have comparable radiant intensity have a lower luminous intensity.

The candela (unit cd) was first defined in the International Units of Measurement (SI), which also saw the unit's name change from "candle" to "candela." The candela derives its name from the illumination of a "standard candle," but it now has a more precise meaning. The candela measures the amount of light emitted in the range of a (three-dimensional) angular span (Blaise & Pétry, 1968).

2.2 Light Distribution and Colour Dimensions

2.2.1 Colour Measurement

The aim of color measurement is to quantify the visual perception of color in order to describe it objectively. A color measuring instrument defines color numerically in terms of color attributes. Color measurement plays a key role in color management, for example, in measuring the color difference between sample and proof, formulating special inks, etc. A color perception phenomenon is based on three components: a light source, an object, and the viewer, i.e., the human eye. A color is measured as the amount of radiation reflected or transmitted from a color stimulus over the specified wavelength range. The tristimulus values can then be calculated by multiplying the spectral reflectance (or transmittance) factor of the color sample by the spectral power distribution of the light source and the color matching functions (Hoang et al., 2005).

2.2.2 Human Perception

The different wavelengths in the visible spectrum can also directly stimulate different colors in the human visual system. A color stimulus generally has a spectral power distribution that varies with wavelength across the visible spectrum, producing a color or sensation that is a shade of or mixture of the colors. Stimuli containing all the visible wavelengths in roughly equal proportions appear white. Passing white light through a glass prism, which spreads the light out into a spectrum of colors. However, white light can also be produced by superimposing discrete monochromatic lights. For example, white light can be produced by

superimposing red, blue, and green lights in certain proportions, known as the trichromatic theory of human color vision (Maloney & Brainard, 2010; Zhang et al., 2013).

2.2.3 Colorimetry and CIE System

The fields of science and technology known as colorimetry are used to measure and physically characterize how people see color. Visual colorimetry and photoelectric colorimetry are the two major categories of colorimetry. By using visual colorimetry, concentration can be determined by visually monitoring the target solution's color change. Since it is difficult to discriminate between different colors with the unaided eye, photoelectric colorimetry has higher measuring precision. Photoelectric colorimetry is used in many different sectors and makes use of tools like spectrophotometers and photoelectric colorimeters, which are more accurate at determining concentration and at resolving color changes. The foundation for estimating the visual matching between two color stimuli is provided by colorimetry. In 1931, the CIE, the International Commission on Illumination, established a colour specification system. The 1931 CIE system is derived from a series of colour-matching studies to define a standard observer. (Clydesdale & Ahmed, 1978).

2.2.4 Color Models

Colour spaces (RGB, LAB, XYZ, CMYK, HSB/HSL, YUV and others) are theoretical three-dimensional constructs that facilitate the identification of colours and their characteristics. They are created by defining colour-variation in terms of three quantifiable range-values and using this framework to determine the placement of a colour spectrum within a three-dimensional space.

2.2.4.1 RGB Color Model

It's common to use a unit cube to represent the color space for software display technologies. Each of the three orthogonal coordinate axes in a 3-dimensional model is given a color (red, green, or blue). Below is a picture of one such cube, along with several important colors and their locations (Figure 3.). The colors on each quadrant of the color cube vary from those in which that element has no contribution to those that are fully saturated. The color cube is solid, and any location (or color) inside it is described by a triple of three numbers, or an R, G, and B. All of the gray scales are represented by the cube's diagonal line, which runs from black to white (0, 0, 0 to 1, 1, 1). The red, green, and blue colors are each represented by one

of the three dimensions. Several color palettes, such as those in the 0-256 range, are used in practice by various computer software. In other words, the RGB cube displays less colors than what our eyes can see because it is within our perception space. The RGB model is frequently employed in digital goods and is extensively utilized in manufacturing output (Fan et al., 2021).

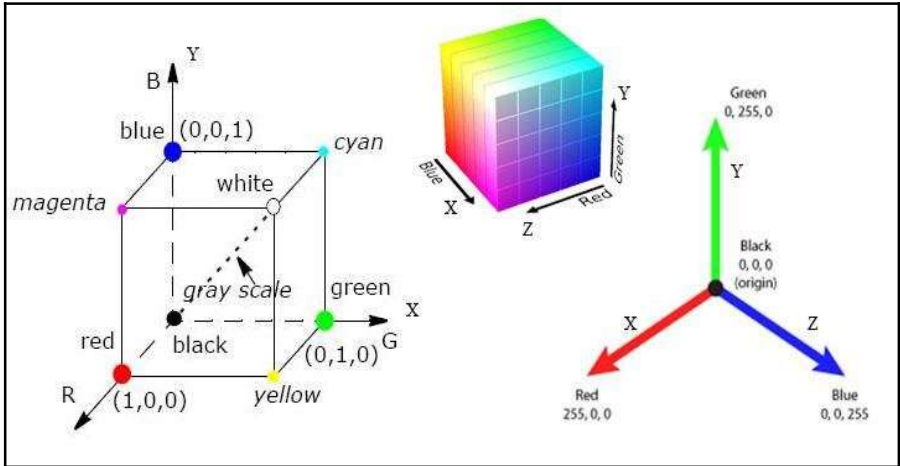


Figure 3. 3-Dimensional RGB Color Distribution (Bhatti et al., 2021)

2.2.4.2 CIELAB Colour Model

Thousands of colors are perceived by the human eye. Nevertheless, it won't always be capable of identifying colors from one another properly. Depending on your viewing position and lighting, you might sense variations in things that are the same color as one another or interpret two colors that are only slightly different as the same. When discussing color, this makes communication difficult. Manufacturers and designers require methods to measure a color's attributes and establish the numerical difference between shades in order to consistently replicate the exact desired hue.

The three components that the CIELAB color system employs to assess true color and compute color differences are represented by the letters L*, a*, and b* in the CIE acronym. Whereas a* and b* indicate chromaticity with no set numerical bounds, L* represents brightness on a scale of 0 to 100, ranging from black to white. Negative a* is correlated with green, positive a* is correlated with red, negative b* is correlated with blue, and positive b* is correlated with yellow (Figure 4.).

CIELAB, or CIE $L^*a^*b^*$, is a device-independent, three-dimensional color space that enables accurate measurement and comparison of all perceivable colors using three color values. In this color space, numerical differences between values roughly correspond to the amount of change humans see between colors. The International Commission on Illumination (CIE) developed the $L^*a^*b^*$ color model in 1976 with the intent of creating a standard for color communication. When creating the CIELAB color space, the CIE drew inspiration from the CIE 1931 XYZ color space, as well as the Munsell color system. All of these models use three data points to define and plot a color (Zhang & Wandell, 1996).

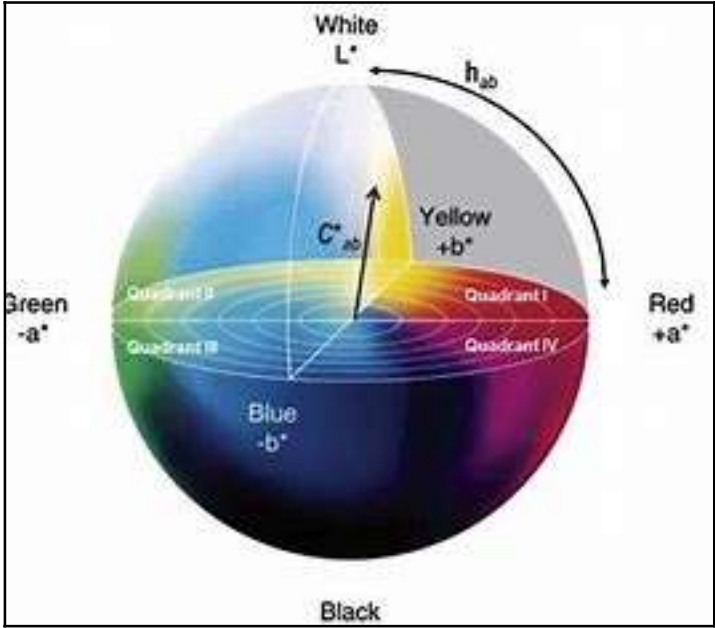


Figure 4. CIELAB Color Sphere. (Sant’Anna et al., 2013)

2.2.4.3 CIE 1931-XYZ Color Model

The first technique for describing light colors or basic colors scientifically, the CIE XYZ color space, was created in 1931 by the International Commission on Illumination. It was the initial definition of color that was broadly accepted as an international standard, and it continues to be the "best model" today. The three different types of color-sensing cells that make up the retina of our eyes are activated to varying degrees, or CIE XYZ values, which are typically defined between 0% and 100% (Figure 5.).

The CIE XYZ was created so that the value of Y served as a representation of a color's brightness and employed the values of X, Y, and Z. To be able to plot the colors on the CIE gamut diagram, the values of X, Y, and Z were utilized to obtain the variables x and y. It is more difficult to represent the CIE XYZ color space as a solid than the RGB color cube. Nonetheless, it would presumably resemble the RGB color cube rather closely, but with obvious color aberrations (Viscarra Rossel et al., 2006).

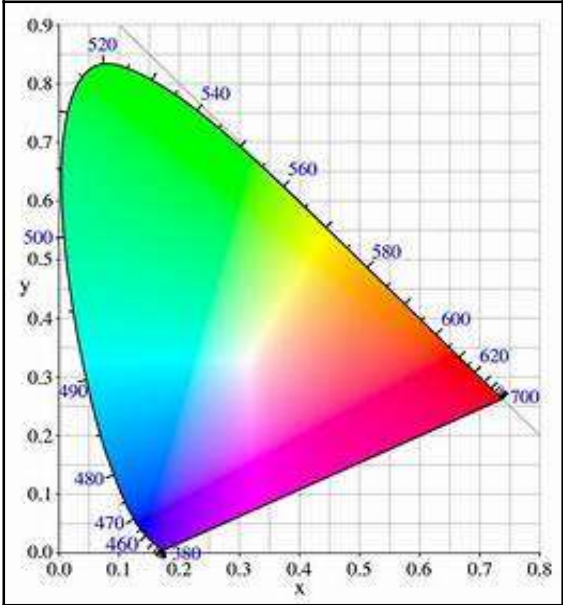


Figure 5. CIE XYZ 1931 Color Space(Kuehni, 2001)

2.2.4.4 CMYK Color Model

CMYK (cyan, magenta, yellow, black), which is made up of three secondary colors: cyan, magenta, and yellow (Figure 6b.). It is a subtractive color model as opposed to RGB since the final color is produced by taking the basic colors away from a white background. To increase the density range and enable the created color's accessible color gamut, black or the key (K) is added. Similar to RGB, CMYK is a tool-dependent color model, which means that the features of each data gathering equipment may change the values that are recorded. In simple terms, various scanners or cameras may provide different registered color intensities. Color intensities with 8 bits of color depth ranged from 0 to 255. For example, absolute white is a combination of [0 0 0 0] in the CMYK color model (Cantrell et al., 2010).

2.2.4.5 HSV Color Model

The hue (H), saturation (S), and value (V) components of the HSV color model are three separate parameters that together make up a multidimensional description of the color rainbow. The color is defined by the hue component as an angular value between 0° and 360° . For instance, the coordinates for red, green, and blue are 0° , 120° , and 240° , respectively. The degree of saturation or chroma (S), commonly referred to as purity, denotes the level of color, which can range from 0 to 100% or 0 to 1. From 0 to 1, where 0 denotes complete black and 1 denotes 100% luminosity with no black incorporated at all, the value of V specifies the brightness or strength of the color. Figure 6c., shows an example of a color geometric cone that can be used to represent these three elements, where hue is represented by a specific point on the color wheel. The height of the color combination cone is used to represent value, while the cone's radius represents saturation. (Thajee et al., 2018)

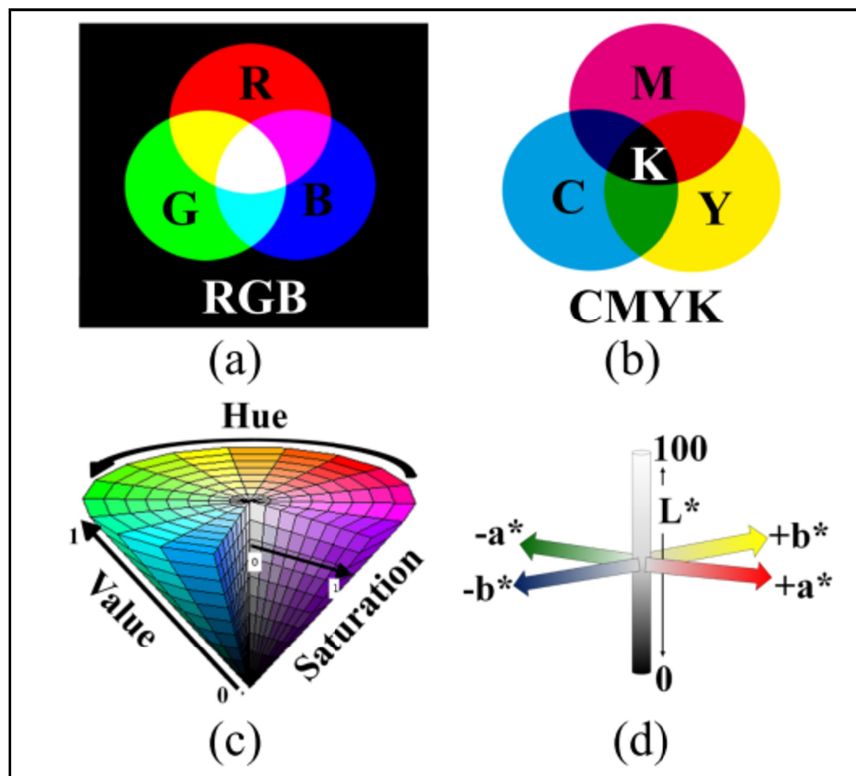


Figure 6. Schematic Diagram among the a RGB, b CMYK, c HSV, and d CIELAB Color Models. Source: (Phuangsaiejai et al., 2021)

2.2.5 Digital Color and Computer Vision

Computer vision is an understanding of chromatic light by electronic/digital, as opposed to biological perception. Because of this, human vision is not described in detail, only the physics of digital sensors are. The collection of images and handling are the two phases that make up computer vision. Measured response spectra showed that these digital cameras are basically three-band radiometers. The response values in the red, green, and blue bands, quantified by RGB values of digital images of the water surface, were comparable to measurements of irradiance levels at red, green, and blue wavelengths of water leaving light.

2.2.5.1 Image Capture and Processing

Digital cameras and RGB values use an array of complementary metal oxide semiconductors (CMOS) to collect high-resolution light intensity data. Each detector in the array acts as a small light sensor (i.e., produces a voltage proportional to the amount of light incident on the detector). A color camera is simply the same detector array covered by a Bayer filter. The Bayer filter has a repeating pattern of colored filter elements. This provides spectral information in the form of large bands in the red, green, and blue portions of the visible spectrum. Using the amount of light measured by each detector, each pixel is assigned a red, green, and blue (RGB) value between 0 and 255 (Wilkes et al., 2016). The Bayer filter is transparent to infrared light; therefore, cameras have an additional infrared filter to prevent infrared light from reaching the detector array (Figure 7).

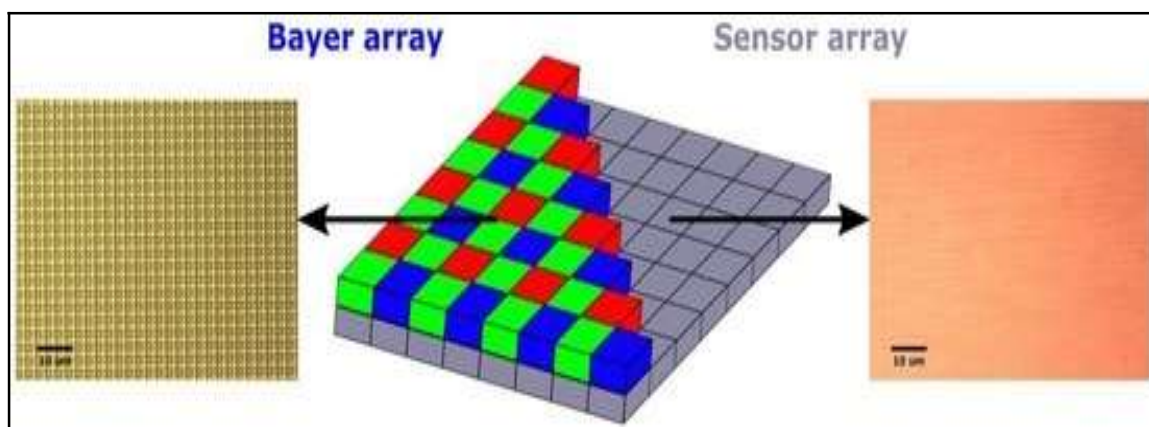


Figure 7. Bayer Filter Array and its Positioning on the Photodetector Array of Image Process (Wilkes et al., 2016)

Electronic image capture corresponds to film photography in that it records a picture of an area or thing by using changes in photo-sensitive material. Digital sensors, on the other hand, provide electrical output from internal arrays of photo-sensitive cells rather than a chemical foundation. Red, green, and blue are the basic additive colors of chromatic light, and there are three different types of cells that measure each of their respective wavelength ranges (Figure 6). When a cell group is exposed, they produce electrical output proportionate to the brightness and color of the light. This electrical output is then estimated as the color value of a single square subspace of the image utilizing additional information from the neighboring cells.

2.3 Water Quality Parameters

2.3.1 Water Quality

Manipulation of water resources for economic evolution and human support circumstances have all suffered as an outcome of declining water quality and ecosystem health. It has grown to be one of the most significant obstacles to ensuring sustainable development in the impacted territory. It is difficult to simply assert if water is excellent or terrible; analytical tests are needed to describe water quality. Therefore, the decision is often based on the use of the water, whether it is for consumption, agriculture, or some other purpose. Communities are also at health risk when there is poor water clarity.

Serious environmental and ecological difficulties must be adequately addressed in order to progress toward sustainable development, notwithstanding the global economy's rapid growth and the crucial role that technology plays in these issues. If sustainable water development is to be realized, the current universal issue of water resources must be incorporated into citizen principles and procedures. Hence, the role of citizens in water management for water quality is to set the intention for all stages of the regime, direct surface water regulatory processes, and implement environmental management systems. Therefore, technology dependence is crucial; it requires a green and digital approach (Jiang et al., 2020).

2.3.2 Nitrate

Nitrogen is one of the most important nutrients for guaranteeing food supply and security. Besides, more nitrogen fertilizers are required due to the population's constant growth. For

both plants and animals, nitrogen is a crucial nutrient, and it can be found in the environment as nitric oxide, nitrite, and nitrate. These are consistently found in typical samples, including dietary, environmental, and biological samples (Eickhout et al., 2006) . However, Swaney et al. (2018) justified that nitrate is present in water both naturally and as a result of exogenous inputs, such as animal and human waste, soil organic matter runoff from agricultural soils, and soil runoff from other types of soil. The main causes of nitrate contamination of surface water resources are anthropogenic activities and uncontrolled discharges from businesses, farms, and sewage treatment facilities (Quemada & Gabriel, 2016). When these growths disintegrate, they add to the organic load in the water body and may deplete dissolved oxygen, which may result in acute deoxygenation. The badsmelling, black heaps of decaying material deposited on the shores have been a source of public complaint for many years and have caused the loss of many aquatic species. (Carolina, 2002) concluded that surface water eutrophication has emerged as one of the main barriers to sustainable economic development.

Ward et al. (2018) described that consumption of water contaminated with nitrates has only been strongly associated with the presence of "blue baby syndrome" in infants (which may eventually lead to mental retardation) as an acute effect, leaving out other side effects that require attention, despite the fact that nitrates have been determined to be carcinogenic components due to the endogenous formation of N-nitroso compounds. Additionally, Shao-ting et al. (2007) verified that thyroid gland can be affected by a variety of pollutants known as endocrine disruptors, which are substances that can interfere with the synthesis of hormones. To date, it is known that nitrates may disrupt the amount of iodine uptake, frequently leading to hypothyroidism and affecting the metabolic functions of the organism at all stages of development, placing a significant burden on the health of those exposed. Mar & Qbal (2007) highlighted the impact of consumption of water contaminated with nitrates and its effects on the thyroid gland in humans, concluding that nitrates could act as a true endocrine disruptor.

In the United States, the allowable contamination threshold for nitrate in public drinking water sources is 10 mg/l as nitrate-nitrogen. This amount is about similar to the World Health Organization's (WHO, 2008) nitrate guideline of 50 mg/l (multiply $\text{NO}_3\text{-N}$ mg/l by 4.427). Nitrate can be found in a variety of foods, with the largest concentrations seen in various green foliage and root crops. Regulation is constantly restricting mineral nutrients flows in

order to reduce their influence on surface waters. Similarly, nitrate releases must be kept to a minimum. The natural nitrate concentration in surface waters is normally less than 4.43 mg/l, while the maximum allowable level of nitrate in drinking water is 50 mg/l. In surface waters, standard values varied from 0.005 to 0.5 mg/l nitrate-nitrogen (USEPA, 1994). The amounts can rise based on the geology of the area, land management, and fertilizer application. Nevertheless, except at extremely high levels nitrate is relatively non-toxic to fish and poses no health risk. (Stone & Thomforde, 2004)

2.3.3 Phosphate

Almost all of the phosphorus (P) in water is in the form of phosphate (PO_4). As a vital ingredient for living creatures, phosphorus (P) plays an important role in the growth of aquatic life. Nevertheless, in an aqueous environment, a fully oxidized version of phosphorus, i.e., phosphate, plays a significant role in the eutrophication cycle. Phosphates are classified into three types: orthophosphates, condensed phosphates, and organic phosphates. Phosphates are usually referred to as orthophosphates in water quality assessments. Abnormal phosphate levels caused by the widespread use of phosphate-based insecticides, fertilizers, beverages and detergents, as well as purposeful or unintentional improper human impacts, are recognized to be hazardous to natural waters. This eventually leads to a decrease in the amount of dissolved oxygen in water, followed by the destruction and rotting of marine animals and the deterioration of water quality (Heidari-Bafroui et al., 2021).

Surface water phosphate overloading is a worldwide issue that endangers both the marine environment and human and animal health. Correll (1998) attributed elevations in algal development in surface water to wastewater discharges and farmland run-off fertilizer. He proposed phosphorus as the culprit and anticipated lake algal outbreaks. Since then this threshold has been recognized as crucial, despite numerous exceptions. The role of phosphorus in the occurrence of algal blooms has received a great deal of attention. In surface water, phosphorus is coupled with both living and dead microscopic matter. Even though phosphorus is an essential plant ingredient that is often in short supply, contributing phosphorus to water stimulates plant (algae) development. Algal growth can be either unwanted, as in pure streams, or beneficial, as in fish farming ponds. Surface waters typically have a range of 0.005 to 0.5 mg/l (Lazur et al., 2013)

2.3.4 Source of Nitrate and Phosphate

2.3.4.1 Agricultural Activity

Cropping system and fertilizer management inputs are two manageable factors that have varying effects on nitrate losses, according to Randall & Mulla (2001). Furthermore, Liu et al. (2022) demonstrated that these row crops leak significantly more nitrate when compared to perennial crops; at the moment, it is difficult to grow many perennials with adequate economic returns. However, Randall & Mulla came to the conclusion that enhancing fertilizer management by delivering nitrogen and phosphate at the optimal rate and timing, as well as properly crediting past legume crops and animal manure treatments, will also result in decreased nutrient losses. Furthermore, studies have indicated that, when compared to nutrient management techniques, tillage systems have little impact on nitrate and phosphate losses. Moreover, Mng'ong'o et al. (2022) studied, overuse of fertilizers necessitates the acquisition of more land away from sensitive areas for the public's and the environment's health. In addition to, excessive and careless fertilization, build-up, and eutrophication to the water.

Manure and wastewater runoff from animal farms made up more than 50% of the nitrate in surface water, which is well-known potential source of many different pathogenic organisms that can sicken people, especially through drinking contaminated water according to (Cao et al., 2022). They noticed that residential and livestock operations consistently release large amounts of contaminants into natural waters, causing physiochemical and biological changes in surface water. Additionally, it increases water turbidity, which contributes to contamination of the water. Besides, they concluded that physical and chemical changes brought on by such anthropogenic activities in lakes may have contributed to fish mortality in lakes.

2.3.4.2 Urban Activity

Water use for drinking, industry, agriculture, recreation, and other reasons is negatively impacted by nutrient enrichment. Rout et al. (2021) justified that household dirty water management is ineffective due to the massive amounts of inorganic garbage evacuated from homes, hotels, restaurants, schools, and retail center on a regular basis. Peng et al. (2022) stated that urban activities are the primary sources of phosphorus and nitrogen in the aquatic environment. They concluded that non-point nutrient inputs are difficult to quantify and control because they result from activities spread across large areas of land and are

unpredictable in time due to weather influences. In addition to what Hamilton et al. (2016) observed, these nutrients have a variety of negative effects on aquatic ecosystems, including toxic algal blooms, oxygen depletion, fish kills, extinction of species crucial to trade and recreation, loss of coral reefs and aquatic plant communities, and others.

2.3.4.3 Land Use Change

Huang et al. (2014) justified that the land on the earth's surface that was converted from forest vegetation to farms and urban areas now supports crucial human livelihoods. Moreover, essential natural resources and ecosystem services are required as the population grows. However, Yona et al. (2022) agreed that excessive growth and extensive farming disrupt ecological integrity, deplete soil fertility, cause significant soil degradation, and discharge large amounts of fertilizer and debris into aquatic ecosystems. Furthermore, Yona et al. added that untenable field management, such as habitat destruction, forest loss, sedimentation, poor crop management, ongoing ecosystem change, and human impacts, causes poor water quality and quantity, limits access to food, and thus affects plankton abundance.

2.4 Water Quality Measurement

2.4.1 Analytical Techniques

To slow and reverse the deterioration of water quality, it is necessary to strengthen the monitoring, evaluation, and governance of surface water quality. Analytical method water quality monitoring mainly relies on collecting water samples on site and sending them to the laboratory to measure various water quality parameters. This Analytical method has the advantage that many different water quality parameters can be measured. Analytical techniques in laboratory practice are characterized by high precision, accuracy, sensitivity, and selectivity (Das et al., 2022). However, Pires et al. (2014) criticized the disadvantage that water quality data can only be collected at limited time points, and the sampling interval is usually long. This is because such sampling usually requires professional equipment and trained technicians, and many of the instruments are expensive, heavy, inconvenient to carry, and labor-intensive. The collection of water samples, followed by sample preparation and laboratory analysis, is complicated and expensive.

2.4.1.1 Colorimetric Technique

It is usual practice to employ a color generating reagent in conjunction with a colorimetric method to assess the proportion of a chemical substance in water. When the desired component and a particular reagent combine, a change in color happens. The key benefits of this technology are that it is affordable to analyse and is unique to different molecules. Scientists created a colorimetric method for estimating the amount of soluble phosphate in saltwater. It became the accepted method for colorimetric phosphorus determination. In this procedure phosphate ions react with an ammonium molybdate reagent solution containing ascorbic acid and antimony (III) to create a blue phosphomolybdate complex (Acta & Muri, 1962).

Sajidu (2007) used the salicylate and vanadomolybdophosphoric acid colorimetric methods to measure phosphates and nitrates in surface water samples. He emphasized that the proportion of the colored component in the mixture is related to the assessment of the light adsorption capability of the system (a colored solution). The rate at which the intensity of monochromatic light diminishes as the concentration and thickness of the transparent material (a colored solution) increase is directly related to the light's intensity. The colorimetric approach relies on determining the optical density of the colored substance, which absorbs most strongly at 520 m, and the interaction of a water sample with specific reagents. The findings were found to be precise and repeatable. However, analytical methods call for costly machinery and labor-intensive processes. The colorimeter is not cheap. Measurements might be challenging on surfaces that reflect light. In the UV and IR spectrums, it is ineffective. A colorless compound is not practical and is time-consuming.

2.4.1.2 Ultraviolet-Visible Technology

Human economies and development are directly correlated with water resources. The precise and fast determination of the primary water quality metrics has emerged as a recent research issue due to the deterioration of the environment for water resources. According to Alves et al. (2018) research, ultraviolet-visible spectroscopy is a useful instrument for both qualitative and quantitative evaluations of pollutants in water sources. Ultraviolet-visible technology, combined with a diverse array of advanced technological innovations, has evolved into a powerful and effective method for detecting contaminants in aquatic environments due to the benefits of being highly accurate, having high recognition efficiency, requiring non-

destructive sampling, and providing environmental protection. Additionally, they provided justification for this by outlining the UV-Vis spectroscopic detection concept for water quality metrics as well as the approach for modeling and spectral data interpretation. The emission or absorption spectra of substances are used in spectroscopy as a tool for substance identification and quantitative measurement. However, Guo et al. (2020) have been criticized because the equipment used is large and expensive a large number of reagents are required, resulting in additional contamination.

2.4.1.6 Fluorescence technique

Fluorescence technology is a spectroscopic examination method in which the sample is electronically excited by light of a particular wavelength and subsequently emits energy at various wavelengths. The intended analyte's quantitative and qualitative characterization is made possible by the wavelength range. In order to assess the concentration of phosphate, Kröckel et al. (2014) developed a tiny fluorescence detector. The excitation light's disturbance could be reduced by the detector's ability to capture significant amounts of uniformly emitted light in all directions. Using a fluorescence probe, Zhao et al. (2011) described a simple procedure for phosphate determination. The carbon dots used in the probe were tuned for europium. Analytical procedures that use fluorescence are easy and quick. Variations in temperature, sample turbidity, pH, photochemical degradation, and direct sunlight intensity all have an impact on fluorescence intensity. Substances that absorb a portion of the excitement or emit energy may also have an effect.

The security and purity of water depend greatly on the proper assessment of phosphate. Flavin mononucleotide, an intracellular form of vitamin B2, was employed as a fluorophore. For the sensitive and targeted detection of phosphate, a novel "off-on" fluorescent sensing technology was created, and it demonstrated great fluorescence response and strong discrimination for phosphate recognition. For the management and routine analysis of nitrates and phosphates, both in water and soil samples, a straightforward and sensitive analytical technique is preferred for the aforementioned reasons. This is despite the fact that sophisticated instruments and skilled personnel are typically required for such sampling, and many of the tools are costly, large, awkward to transport, and labor-intensive (Xu et al., 2023).

2.4.2 Remote Sensing Technology

2.4.2.1 Satellite Water Quality Detection

An extremely useful method for keeping track of water supplies across various temporal and spatial scales is remote sensing. Rapid and widespread monitoring of inland and coastal water quality occurs through the use of remote sensing and near-surface water quality sensors. The development of satellite remote sensing technology provides a feasible way to monitor water quality across large areas and long time series, and to further discover the temporal and spatial distribution characteristics and migration paths of pollutants. Nevertheless, its application is strongly affected by the satellite revisit period, remote sensing data resolution, and cloud coverage, among other factors. Because shallow water and land borders affect the photos, coastal regions and interior waters cannot employ satellite spatial resolution, which is useful in shelf seas. Such areas require the use of in-situ or aerial-mounted equipment. Currently, the optical properties of natural waters are measured using narrow-band, multispectral radiometers to provide data on a variety of water quality indicators, including chlorophyll, mineral suspended sediments, and yellow material. However, it could be expensive to use relatively complicated multi-spectral sensors (Abdelmalik, 2018).

Today, many satellites with high enough resolution have been used in water quality monitoring studies. He et al. (2008) concentrated on the water quality assessment of surface water, which could serve as a secondary supply of drinking water. Water quality recovery models were constructed and assessed for water quality indicators comprising total nitrogen, nitrate nitrogen, total phosphorus, and dissolved phosphorus using a remote sensing (RS) technique using Landsat 5 Thematic Mapper (TM) data. The findings demonstrate that in moderately contaminated surface water with a low remote sensing reflectance, there is a statistically relevant link between each water quality metric and remote sensing information. It was possible to retrieve the nitrate nitrogen content using the right sampling technique for pixel digital numbers and multiple regression algorithms, as well as the concentrations of total nitrogen, dissolved phosphorus, and total phosphorus.

Investigators of water resources may be better able to monitor surface waters with the help of remote sensing data. The qualitative characteristics of waterbodies, such as suspended particles, colored dissolved organic matter, and chlorophyll a, have been extensively measured using remote sensing technologies (Gholizadeh et al., 2016). Olmanson et al. (2013)

collected pictures with excellent both spatial and spectral resolution for use in evaluating optically active water quality properties of surface water using airplanemounted hyperspectral spectrometers. Images were obtained produced for turbidity, suspended particles, chlorophyll, and other water clarity indicators to determine water quality. They investigated the use of air carrier remote sensing devices as a practical means of gathering data to assess surface water's visually active water quality parameters pertinent to the problem of water deterioration. Last but not least, a better selection of spectral bands than those offered by Landsat is required to measure conditions of water quality other than clarity. Although the MERIS and MODIS satellite sensors have these bands, their low spatial resolution means that they are only useful for very large water bodies. Song et al. (2012) also used a For the distant determination of total phosphorus, chlorophyll-a, and turbidity using specified sensitive spectral parameters, a hybrid approach integrating genetic algorithms and partial least squares(GA-PLS) was developed.

Midland water quality contamination is viewed as a significant environmental issue. And through recovery of visually effective water quality metrics like chlorophyll-a, space-based remote sensing (RS) has become a significant source of data for determining the trophic condition of non-coastal waters. Nevertheless, the application of remote sensing approaches for a global evaluation of the trophic condition of inland waters. Based on Moderate Resolution Imaging Spectroradiometer (MODIS) imaging and the Forel-Ule index, Wang et al. (2018) created a new remote sensing method to evaluate the trophic condition of worldwide upcountry water bodies. First, the natural water color range from dark blue to yellowish-brown was divided to determine the FUI using MODIS data. Then, using in-situ data and MODIS outputs, the connection between FUI and the trophic status index (TSI) was determined. In the FUI-based trophic status evaluation, colored dissolved organic matter (CDOM)-dominated systems were distinguished using the water-leaving reflectance at 645 nm band. The FUI-based trophic state evaluation method was created and used to evaluate the trophic stages based on the findings.

Thiemann & Kaufmann (2000) practised multi-temporal data sets of the LISS-III sensor mounted on the Indian Remote Sensing Satellite (IRS- 1C) and field reflectance spectra have been evaluated for predicting water quality parameters (chlorophyll-a) in lakes. They contrasted their findings to laboratory evaluations of in-situ samples taken. The 678 nm

absorption maximum and the 705 nm reflectance peak were used for quantification from field reflectance spectra. The spectral height of the green peak, supervised maximum likelihood classification, and linear spectral unmixing were three approaches that were contrasted for the assessment of the LISS-III satellite data. Using the Geostationary Ocean Color Imager (GOCI), Huang et al. (2015) supplied greater temporal resolution satellite data to investigate the hourly changes of algae. They investigated a straightforward regional NIR-red two-band empirical method of chlorophyll-a for Taihu Lake's GOCI. Their ability to observe the dynamic properties of algae that change quickly is restricted by the inadequate temporal resolution of satellite data.

Al-shaibah et al. (2021) investigate how Landsat TM5, ETM7, and OLI8 pictures may be used to evaluate the water quality (V-phenol, dissolved oxygen (DO), NH_4 -N, and NO_3 -N) in a lake. Indicators of water quality were investigated using multispectral pictures. Also, all photos had their radiometric and atmospheric corrections made. They all agree that, all in situ water quality metrics, with the exception of DO, were found to be highly associated with one another. The spectral band configurations (blue, green, red, and NIR) obtained from Landsat imagery were statistically correlated with the in-situ measurement techniques (V-phenol, dissolved oxygen, NH_4 -N, and NO_3 -N), and the regression analysis revealed that there are significant connections between both the approximated and obtained water quality from the Satellite image.

With Landsat 5 and Landsat 7 reflectance data (Khattab & Merkel, 2014), straightforward and precise techniques were established for the recovery of water quality metrics for Mosul Dam Lake. In place, assessments of the water quality were made. Temperature, turbidity, Secchi disk, chlorophyll-a, nitrate, nitrite, phosphate, total inorganic carbon, dissolved organic carbon, total dissolved solids, and pH were some of the measures that were obtained. Techniques for picture improvement have been utilized to effectively use the reflectivity spectrum values. The reflectance values of the Landsat 5 and Landsat 7 bands were matched to the field observations using various band combinations using empirical techniques. In general, the analysis's findings indicated a strong relationship between these models and water quality indicators. The assessment between the anticipated characteristics for quality of water and the in-situ measurements revealed that the models utilized had a higher level of predictability.

Padilla-Mendoza et al. (2023) showed that Sentinel-2 photos can be used to create empirical models and predict the level of physicochemical water quality indicators, especially nutrients in the wetland ecosystem. They established significant correlations among the variables affecting water quality. The correlations enabled the determination of statistically significant bands in the multiple linear regression technique implementation to produce empirical water quality models using reflectance data from Sentinel-2 pictures taken on the same monitoring day. The findings demonstrate strong relationships between optically active parameters, such as TSS-Turbidity, which in turn exhibited relationships with optically inactive parameters, such as Turbidity-NO₃ and TSS-DO, as well as non-optically active parameters, such as TDS-NO₃ and TDS-TP, among themselves.

2.4.2.3 Aircraft Water Quality Detection

Aircrafts water quality sensors can cover a large geographic area with high temporal repetition. Bansod et al. (2018) investigated how to recognize water quality metrics in light of the optical dynamic features of the water by utilizing remotely observed information. Water' optical and dynamic qualities can provide a clear picture of its quality, but their accuracy depends on the tests that are taken from various types of water bodies. They used water bodies for which hyperspectral band data was collected using the Airborne Visible/Infrared Imaging Spectrometer New Generation (AVIRIS-NG). Different spectral indices that are useful in assessin chlorophyll-a, turbidity, and aggregate phosphorus were constructed using ground truth data and a collection of spectral bands obtained from hyperspectral imaging.

(Ryu, 2022) showed how an off-the-shelf unmanned aircraft system (UAS, drone) fitted with the additional required hardware connections could be used to track the pH, temperature, electric conductivity (EC), and dissolved oxygen levels of surface water in real time. Moreover, the UAS-based computer system platform for water quality studies appears to be a useful tool for advancing environmental work, particularly for surface water with impairments.

With the addition of cloud cover and higher spatial resolution, UAS images can supplement satellite data. These traits are especially important for mapping tiny water bodies because the resolution of satellites prevents local events from being recognized. Unmanned aerial systems (UAS) have developed into a cutting-edge podium for gathering super-resolution photographs at lower elevations that offers simultaneously high spatial detail (centimeter-scale) and

adjustable temporal resolution (flexible time resolution) at an ever-declining cost (Isgró et al., 2022).

2.4.2.4 Smartphone Water Quality Detection

Remotely sensed and near-surface earth water quality observation sensors are used rapidly and widely to monitor the condition of inland and coastal waters. Smartphone monitoring of water quality by members of the public could offer a real-time assessment of water quality in addition to conventional test samples. Water samples were processed in a laboratory and also collected mobile photographs for comparison, According to Malthus et al. (2020) hydroColor detects RGB reflection and EyeOnWater (IOW) calculates the Forel-Ule scale, which provides a clue as to how the water surface appears visually. They came to the conclusion that while EOW is a stronger software and is better able to accurately and precisely capture the color of water, HydroColor has great promise but is limited by faults in the observing approach and errors in the handling of photographs in the smartphone. Furthermore, by stating that both apps had the ability to generate other water quality parameters from observations of water color that were adequate and quite accessible.

Monitoring natural resources on various time and space scales is made especially easy by remote sensing. Leeuw & Boss. (2018) developed a color smartphone application that assesses the remote sensing spectral response of natural water bodies using a smartphone's camera and supplementary sensors to examine water characteristics. HydroColor makes use of the three-band radiometer found in the smartphone's digital camera. Three photos must be gathered in order to meet the standards for radiance. To obtain the card radiance, a gray card image, a sky image, and a water image are required to get the water radiance. The water's reflectance in the broad red, green, and blue wavelength bands is calculated using these photos to monitor the water quality. In contrast to other water quality camera techniques, Hydrocolor's operation is based on radiometric readings rather than image color. As a result, hydrocolor is a potent device for collecting water's optical data through crowdsourcing.

The Nikon Coolpix 885 and the SeaLife ECOshot are two commonly used digital cameras that are utilized as in-situ optical equipment for water quality assessment. In essence, these digital cameras are three-band radiometers, as evidenced by the observed spectral signatures. The response values at the RGB wavelengths of the water leaving light, as measured by the

RGB values of digital photographs of the water surface, were identical to determinations of the irradiance conditions at those wavelengths. Various techniques were used to catch light that was upwelling from beneath the surface while preventing direct surface reflection. When compared to earlier measurements made using more conventional narrow-band radiometers, it was discovered that the connections among water quality metrics and the RGB ratios of photographs of the water surface were reliable. The Harbortronics DigiSnap 2000 time-lapse control was used to handle the camera, which was installed within the enclosure and peered down through an optical lens that was about 10 cm below the edge of the water. Additionally, the authors pointed out that the SeaLife ECOshot is a waterproof digital camera made specifically for taking images underwater. The CP885 and ECOshot response spectra were measured in the UV-1601 double beam spectrophotometer, while the ECOshot was held and operated below the water's surface while shooting photographs (Goddijn-Murphy et al., 2009).

A platform for on-time water quality determination must be rigorously created to ensure that a smartphone application is usable to a certain level, especially given that consumers are a diverse group of individuals with different wants and desires. The outcomes were attained through quality assessment using a modified Goal Question Metric (GQM) approach, such as field testing and surveys. The inspection results demonstrate the real-time water quality management application's excellent levels of effectiveness and productivity, as well as its users' satisfaction. But there were certain issues that needed to be resolved. The internet access must be steady, and the text's sizes ought to be larger. If the GQM model and another accessibility model could be integrated, this usability evaluation may be enhanced. The questions concentrating on customer perception with smartphone apps were created using the GQM model metrics for water quality parameters monitoring phones as a foundation (Bokingkito & Caparida, 2021).

For environmental conservation purposes, phosphate levels in water should be constantly supervised. Therefore, a simple, portable, and accurate instrument is required to assess phosphate levels in the field. In this study, a low-cost dip strip is created for the determination of low phosphate concentrations in fresh and saltwater. In this apparatus, the ascorbic acid reagent was dried on blotting paper to create the detection zone, after which it was followed by a molybdenum technique wet chemistry procedure. To greatly extend the life of the device

and increase the repeatability of its function, ammonium molybdate and sulfuric acid were kept separately in a liquid state. Distilled water and seawater were used to test the gadget (Heidari-Bafroui et al., 2021).

Monitoring water quality is becoming increasingly dependent on crowdsourced findings from smart devices. Nonetheless, ensuring and assessing the quality of public generated data is a critical task. A computation model was developed to transform the photograph's digital numbers (DNs) into a spectral curve, and a set of inexpensive reference cards was created to be positioned in the middle of the image, close to the water's surface. The intrinsic reflectance and DN of the reference card in the image were used to build a non-linear DN-to-reflectance model. The water surface reflectance in the same image was then calculated. The method suggested, which relies on a cellphone camera, may be utilized to accurately and efficiently calculate the remote sensing reflectance and water quality metrics. Crowdsourcing is the process of gathering data, viewpoints, or creative output from a large number of individuals, typically online. Through the use of crowdsourcing, businesses may access individuals with a variety of skills and viewpoints from around the globe while also reducing expenses and time (Gao et al., 2022).

3. MATERIAL AND METHOD

3.1. Research site

In Winter 2023, field measurement was carried out at number four (4) fish culturing ponds (Figure 8.), Gödöllő-Állami telepek (47° 33' 55.53" N and 19° 22' 5.45" E), which are located east of Budapest, Hungary. Moreover, the study site belongs to a temperate region with an average elevation of 267 m above mean sea level. In the bargain, the research area receives an average annual rainfall of 339 mm with an average humidity of 84%, and the annual solar radiation is about 1280 kWh/m² as well. Throughout the year, January is the most humid month in the study area. Furthermore, the research field has a surface area of 750 m² (50 m length by 15 m width) and a maximum depth of 120 cm, while the pond has a capacity of 900 m³ and a flow rate of 15 m³/h (Figure 9.).



Figure 8. Image of Study Area (Gödöllő-Állami telepek). Source: Own

The ponds are fed by Rákos-patak (Rákos-creek). The feeding of the reservoirs always arrives before the effluent of the waste water treatment plant in Gödöllő. The types of fish growing in the area are *Cyprinus carpio*, *C. carpio*, *Abramis brama*, *Carassius carassius*, *Clarias gariepinus*, *Sander lucioperca*, and *Essox Lucius*. However, the water quality in the pond is impure due to internal adulteration sources (aquaculture) and external contamination sources (agricultural and urban runoff) from the surrounding areas.

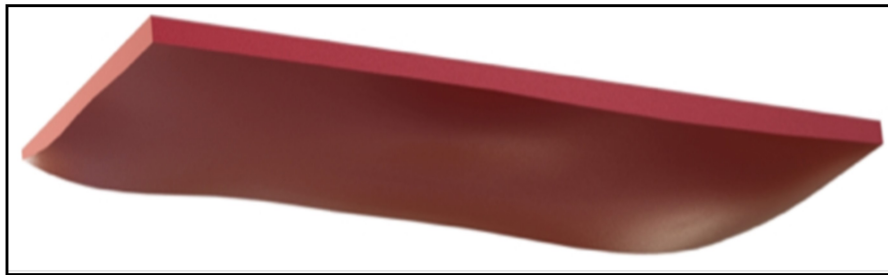


Figure 9. Three-Dimensional Image of the Study Area. (Barczi, 2015)

3.2 Methods and Measurement

3.2.1 eXact iDip Photometer

Conventional measurement was taken by an eXact iDip smart photometer device, which is a pioneering, compact, capable of measuring different parameters, and water-resistant (IP67) tester. It contains a tiny sample jar that fills with the test water and then agitates around the test strip for the particular test to be performed. After a while, pressing the button on the iDip starts a countdown to ensure the test strip has been in the sample for a sufficient length of time, and after that, the photometer uses a 525 nm light source to assess how much light can pass through. The photometer gives two kinds of readings, and a Bluetooth-ready Android mobile phone has a long-lasting built-in sample cell (Figure 10.). Moreover, this excludes the separate cell and modifies the test method, which improves accuracy. As well, the results are finally displayed on the photometer's digital screen and transmitted via Bluetooth to the paired Android smartphone device with the spreadsheet.



Figure 10. eXact iDip Smart Photometer. source: Web 2, n.d.

3.2.2 Photometric test procedures

To determine nitrate and phosphate, the technique for testing the water parameters is straightforward and simple to do. Fill the test cavity with a water sample first, then select the test on the smartphone app and run the process to analyse nitrate and phosphate. Push a button to take a baseline reading of the water without any of the test strips dissolved in it. After that, press the button to start the test, and then wait 20 seconds for the timer to count down by placing the corresponding test sample strip in the test tube and stirring it around in the sample water. Once the timer counts down, you set the strip aside and have to wait 10 minutes and 2 minutes for nitrate and phosphate, respectively. Finally, the water result is displayed on the device as well as on the smartphone (Figure 11.).



Figure 11. eXact iDip Smart digital Photometer Testing Steps
Source: Web 3, n.d.

Check the tests a couple of times. After getting a few of the test results, click on an information link in the app. Since some of the data is calculated based on the results of some of the specific tests, without a full complement of tests, it couldn't give a full water report. The app has a lot of features built into it, definitely with professionals in mind. You can set up profiles of customers, with different test locations within each customer site. You can also capture photographs with your phone and attach them to test results. A series of laboratory tests was conducted to determine the camera's response to light intensity and its spectral sensitivity.

The eXact iDip photometer system offers a truly customized system that's accurate, efficient (saving money and time), and an environmentally friendly device that uses green chemistry. Moreover, this device needs a Bluetooth smartphone device to furnish test results. It will not be enough to provide usable information alone.

3.2.3 Sample Collection for Analytical Analysis

Water samples were collected from the surface of the Pond between December 2022, and March 2023. A total of 31 composite representative samples were collected for this study area and analysed for determination of water quality using a device called the eXact iDip photometer. At this particular reservoir, samples were collected with a 250 ml plastic vessel from three different parts of the reservoir each day from the surface and taken for analysis. Thus, these water samples were collected just from the site's surface. Traditional chemical analyses were applied to two common water quality variables, including nitrate and phosphate.

3.2.4 Image Acquisition

This current thesis focuses on the method that was used to acquire digital images, derive RGB values, and relate measurements to water quality parameters. Android smartphone cameras were used as in situ optical instruments for water quality sensing by taking images.

Photos were collected from the study area parallel to the water sample for analysis. Thirty-one images were grasped from December 2022, to March 2023, and the images were selected for RGB and CIELAB value analysis. During image acquisition, the camera should be pointing toward the water surface at a viewing zenith angle of 40-45, and the viewing azimuth angle should be approximately 135. The RGB color value (0-255) is obtained by uploading the image to a colormeter cellphone application.

To describe the visually-perceived color properties of an image, we do not naturally use the proportions of red, green, and blue components, but rather terms such as brightness, color, and color purity. Within the CIELAB space, a psychometric index of lightness (L^*) and two colour coordinates (a^* and b^*) are defined. The L^* index is related to the luminosity; according to this property, each colour can be considered as equivalent to a member of the

grey scale, i.e., between black (L= 0) and white (L=100). where a low number (0-50) indicates dark and a high number (51-100) indicates light.

3.2.3 Nix Quality Control Sensor

The red, green, and blue (RGB) sectors of an image of a colored sample solution taken by a digital camera, hand scanner, or cellphone camera are used in the new technological method known as digital picture detection. A user's initial perception of an item will be shaped by its color, which is one of the main things they will observe about it. Color scheme has the power to express a brand's personality and even trigger an emotional reaction from the consumer. A visible sense of worth and quality is communicated through color. A product's effectiveness and the bottom line are inevitably impacted by color.

Nix quality control color sensors (Figure 12.) can be easily integrated into the work cycle of any measurement. This is due to the Nix QC's exceptional capability to gauge the hue of practically any substance, including solids, liquids, powders, and gels. High levels of color reliability are provided by the Nix quality management data logger, a reasonably precise and cutting-edge technology product that is also incredibly simple to use. In the old days, this usually meant either hefty testing equipment that was challenging to utilize or traditional swatches that were manually examined.

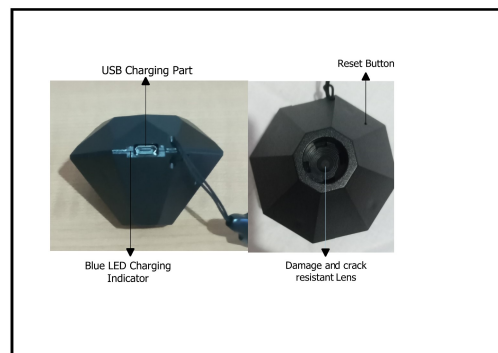


Figure 12. Parts of Nix QC Color Sensor. Source: Own

The use of a digital colorimeter is the current method of color quality control. Despite their incredible precision, these machines are frequently expensive, challenging to use, and limited to a lab benchtop due to their large size and fragile parts. The Nix QC color meter, however, was created with these problems in mind. The Nix QC Color Sensor's user-friendly, easily

carried-out design can guarantee color uniformity throughout a product's lifespan while also having the precision, stability, and inter-instrument concordance to tackle even the most challenging color quality control duties.

3.2.3.1 Toolkit Smartphone Application

The toolkit application, available for Android phones, must be installed on the mobile phone in order to use the Nix quality control device. Manage and keep an eye on the color difference on the research samples while using the Nix quality control device and the Toolkit cellphone application. Using the desired color space range, examine the color variation between both the scanned samples and pinpoint the sample's lightness and hue differences from the reference. The scan will be noted and recorded so it can be later referred to if the sample color doesn't reach your predetermined threshold. Three parameters—the RGB (red, green, and blue) and CIELAB results—are displayed on the mobile application.

3.2.3.2 Nix Quality Control Sensor and Data collection

The Nix QC sensor arrives in a "sleep" state. Connect it to the power supply to make it active. Afterwards, when the Nix QC is charging, a tiny blue light comes on to show that electricity is being provided. Besides, keep the device plugged in to get a full charge. Place your Nix QC flat on any stable, blurred surface after that and begin scanning. For the best accurate readings, keep the device firmly against the material to completely block out ambient light. Be sure the device is charged and awake before intending to access the Nix Toolkit app. Make sure Bluetooth is turned on in your mobile system preferences and activate the Nix QC app.

Place the Nix color quality control sensor next to a smartphone. On your screen, click the dormant Bluetooth icon in the upper left corner (indicating that a device is not connected). If prompted, pick the equipment from the list with the strongest signal. The average time for a connection is 15 to 20 seconds, but it can take up to 60 seconds. When paired, a Bluetooth icon that is active should be visible. After that, collect RGB and CIELAB values from the smart phone application by scanning the water from 16 samples with the Nix QC device (Figure 13.).

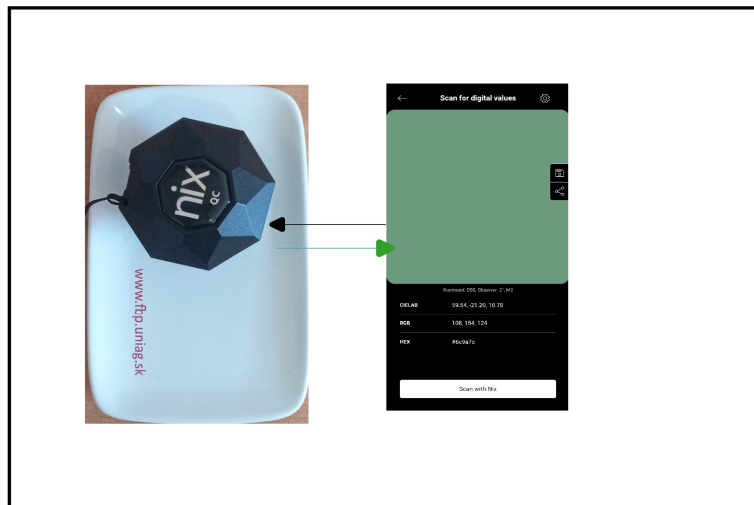


Figure 13. Nix QC Sensor and Toolkit Mobile Application.
Source: own

3.2.4 Color Analyser Smartphone Application

An application called Color Analysis meter which measure the remote sensing reflectance of natural bodies in an image detected by a mobile camera and other digital cameras. Color analyser application leverages the smartphone's digital camera to detect the RGB color value of an object. The application program instructs users to take images using their mobile device's camera in order to calculate the RGB value of the image.

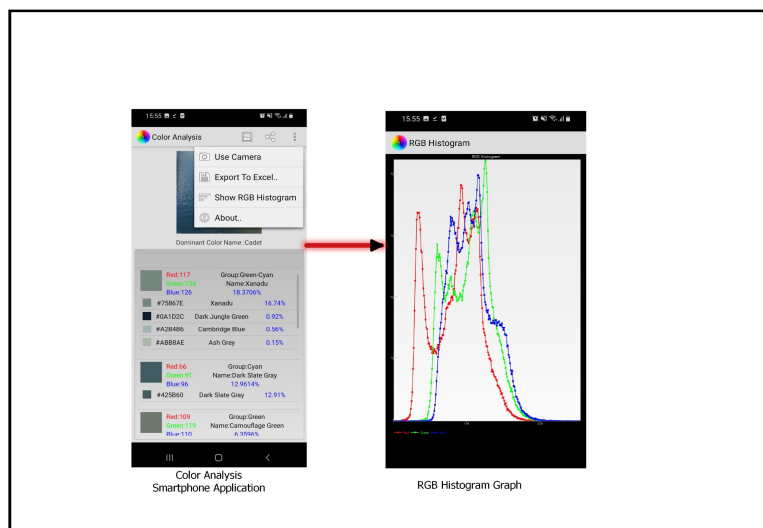


Figure 14. RGB Color Analyser Smartphone Application.
Source: Own

Surface water reflectance in the red, green, and blue color values of the image is calculated by uploading the photos to the mobile application (Figure 14.). Each of the three parameters (red, green, and blue) specifies the color's intensity as a number between 0 and 255. For example, RGB (255, 0, 255) is rendered as red and blue because the red and blue parameters are set to their highest value (255), and the others are set to 0 (green).

3.3.5 Statistical Data Analysis

Data analysis is of central importance in the education of scientists. The Excel features of most relevance to the analysis of experimental data in the physical sciences are dealt with in some detail. The data that I collected was stored in a Microsoft Excel spreadsheet. After gathering all the data from the eXact iDip photometer, Nix color quality, and colormeter phone application, it was also analyzed in LibreOffice Excel.

In order to analyze the data, LibreOffice Excel was used. For all the information gathered from the photometer, the NIX QC sensor, and the Colormeter mobile application of the water reservoir during the season, the minimum, maximum, average, and standard deviation were calculated. The standard deviation to mean ratio (SDV/M) was used in Eq. (1) to calculate the coefficient of variation (CV%). The CV details the variations in nitrate and phosphate levels.

$$CV=(SDV/Mean) * 100 \quad (1)$$

Variation was categorized as little variation (CV% < 20), moderate variation (CV% = 20–50), and high variation (CV% > 50). A correlation and linear regression coefficient were also computed to determine the extent of association between nitrate and phosphate (Verla et al., 2020).

Any statistical association between two variables is referred to statistically as correlation (dependency). In statistics, "correlation" typically refers to the strength with which a pair of variables are linearly associated, even if in its broadest sense it can denote any kind of association. The relationship between nitrate and phosphate concentrations was computed in this study. Additionally, the levels of nitrate and phosphate were correlated using a scattering graph with the red, green, and blue channels that were gathered from the Nix quality control sensor and from the smartphone color analysis application.

The cornerstone of statistical modelling is linear regression. In this thesis, the link between the RGB color results (dependent) and variable concentration (independent) is modeled using a linear technique. The associations between the nitrate and phosphate variables of different concentrations and the red, green, and blue color data are modeled using linear predictor functional equations, whose unobserved model parameters are derived from the data. When the R^2 value is zero, it indicates no linear relationship; when it is 0.30, it is indicative of a weak positive linear relationship; when it is 0.50, it is indicative of a moderate positive linear relationship; when it is 0.70, it is indicative of a strong positive linear relationship; and when it is positive one, it denotes a perfect relationship.

4. RESULT AND EVALUATION

4.1 Photometric Results Analysis

Descriptive statistics for water quality variables calculated from all water sample data are shown in Table 1., including maximum (MAX), minimum (MIN), average (AVG), and standard deviation (STD). The mean and standard deviation for nitrate and phosphate in the winter season are presented below. Nitrate levels recorded for the water bodies did not exceed the limit in the season, while phosphate levels recorded for the surface water quality did exceed the limit in the winter season.

Table 1. Descriptive statistics of water quality variables for 31 water samples collected from study area.

| Statistics | Concentrations | |
|--------------------|----------------|------------------|
| | Nitrate (mg/l) | Phosphate (mg/l) |
| Minimum | 2.93 | 0.14 |
| Maximum | 16.77 | 9.91 |
| Average | 7.79 | 4 |
| Standard Deviation | 4.36 | 3.09 |
| % CV | 55.95 | 77.25 |
| Correlation | 0.05 | |

With regard to the average values of 31 samples for nitrate and phosphate concentrations that were determined with an analytical instrument photometer, the water quality parameter threshold limit was responsible for algal blooms in the water reservoir during the growing season. The gap was small and indicated that the reservoir was not seriously polluted. The results revealed that nitrate and phosphate ranged from 2.93 mg/l to 16.77 mg/l and 0.14 mg/l to 9.91 mg/l, respectively (Table 1.). It can be seen that the maximum values are not very high compared to the average in both nitrate and phosphate (Figure 15.). This is due to the fact that the water samples were collected frequently from one reservoir. On the other hand, the minimum values are fairly small, most of which were retrieved from samples distributed in the central part of the study area. The reservoir showed high variations for both nitrate and phosphate in season (Table 1.). These samples were very valuable for modelling, as they were useful in extending the confidence interval of the color models and ensuring the significance of statistical regression algorithms.

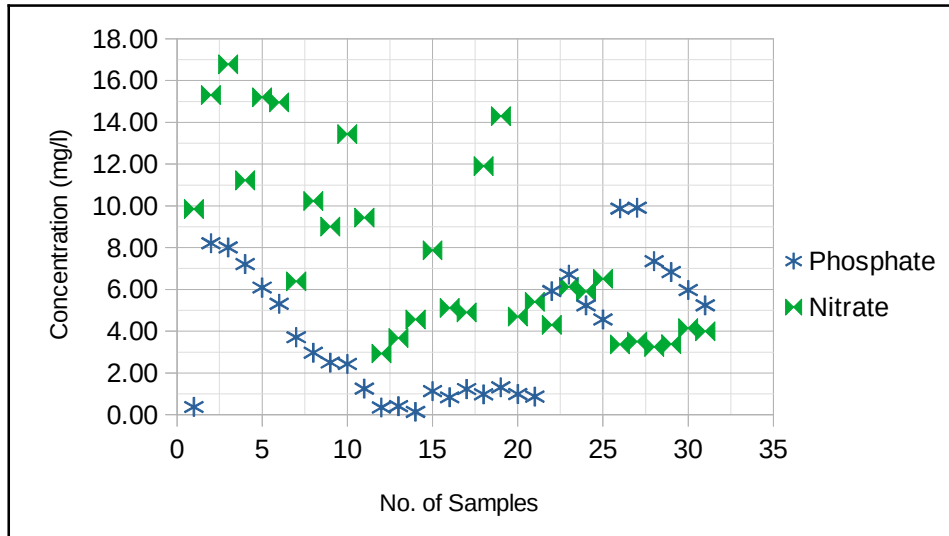


Figure 15. Nitrate and Phosphate Concentration Graph.

The correlation between nitrate and phosphate concentrations was computed in this study. Additionally, in Figure 16., the power relation between nitrate and phosphate was very weak (0.05). These two variables The relationship between the nitrate and phosphate concentrations recorded in the reservoir in the winter season was analysed using linear regression analysis, as presented in Figure 16. A positive relationship generally indicates similar contamination sources. In this study area, nitrate and phosphate concentrations showed a no relevant linear relationship ($R^2 = 0.003$).

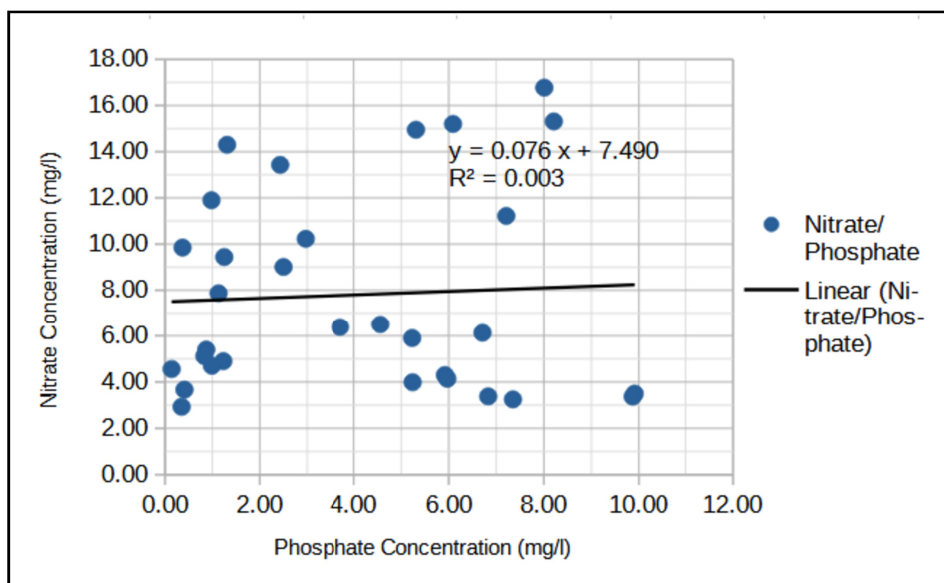


Figure 16: Correlation between Nitrate and Phosphate Concentration.

4.2 Nix Quality Control Result Analysis

In the research area, the red, green, and blue (RGB) sectors of the image of a colored sample solution detected by NIX QC from the water sample during the winter season for red, green, and blue (RGB) colors had an average value of 171, 175 and 163, respectively (Table 2.). The highest color value recorded was for green (191), and the lowest result obtained was for blue (147). The highest standard deviation attained from blue and the lowest from red were 6.32 and 2.99, respectively. The pond showed a very small coefficient of variance between the red, green, and blue color results, which ranges between 147 and 191. (Table 2.).

Table 2. Statistical analysis for RGB color values obtained from NIX QC sensor.

| Statistics | NIX QC colour values | | |
|--------------------------------|----------------------|------|-------|
| | R | G | B |
| Minimum | 159 | 167 | 147 |
| Maximum | 181 | 192 | 182 |
| Mean | 171 | 175 | 163 |
| Standard Deviation | 5.1 | 7.07 | 10.32 |
| % CV | 2.99 | 4.03 | 6.32 |
| Correlation (PO ₄) | -0.38 | 0.92 | -0.26 |
| Correlation (NO ₃) | -0.24 | 0.13 | 0.89 |

From the study area 31 water samples were detected by nix color quality control sensor. The RGB color result distribution ranges between 150- 200. As shown in figure 17., the green color value was dominant over red and blue. There is a small gap among the color values which shows a lower variance and the brightness of the water color was 71%, that indicates the water was some how clear. The green was dominant over red and blue colors. Thus, the highest peak was recorded from green and the lowest recorded from blue.

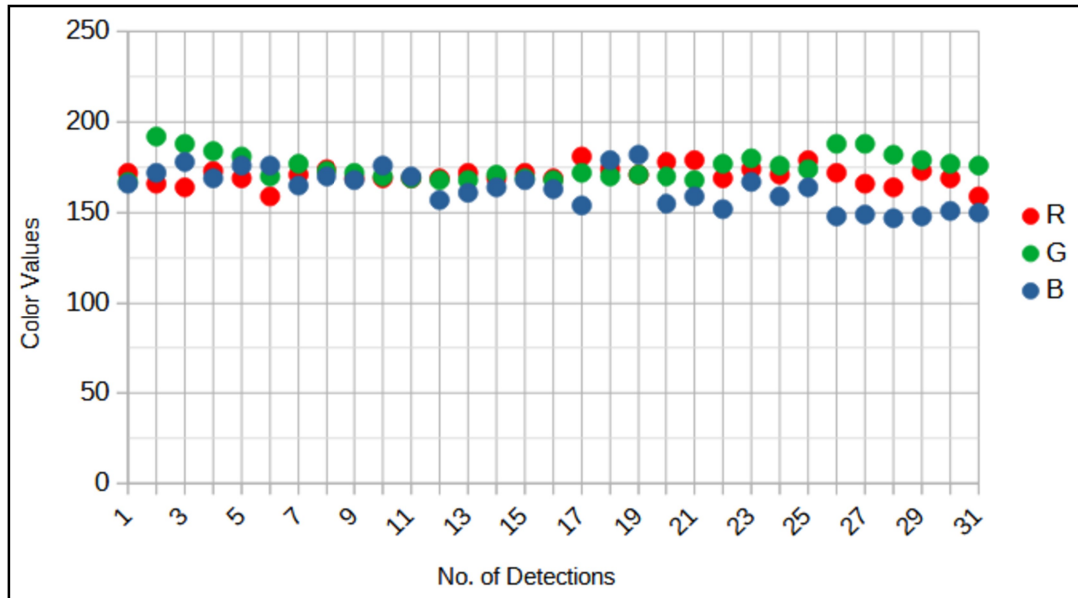


Figure 17. Nix Quality Control Sensor RGB Color Values Scatter Graph.

The values of nitrate and phosphate concentrations that were determined by the eXact iDip photometer were generally associated with the color values of green and blue in waters respectively. A statistical analysis was performed among the nitrate and phosphate parameters and color results. Both nitrate and phosphate were highly correlated with green (0.91) and blue (0.89) color values and negatively correlated with red (-0.38) color values that were detected with the nix quality control sensor. The photometer results varied from 2.93 mg/l to 16.77 mg/l and 0.14 mg/l to 9.91 mg/l for nitrate and phosphate, respectively, which indicates a significant power relation between blue and green with nitrate and phosphate concentrations, respectively (Table 2.).

A linear regression analysis was also computed to determine the extent of the association between nitrate and phosphate. A linear regression correlation coefficient between phosphate and nitrate concentration with RGB color results is displayed below in Figure 18. Nitrate concentrations show a strong positive linear relationship with blue (NO_3/B), and its regression coefficient was $R^2 = 0.80$, but a weak positive linear relationship was obtained from red and green with $R^2 = 0.06$ and $R^2 = 0.02$ respectively. However, phosphate concentration with green (PO_4/G) shows a strong positive linear relationship with $R^2 = 0.86$, while the red and blue color results showed a weak positive linear relationship with $R^2 = 0.14$ and $R^2 = 0.07$, which confirmed this relationship (Figure 18.).

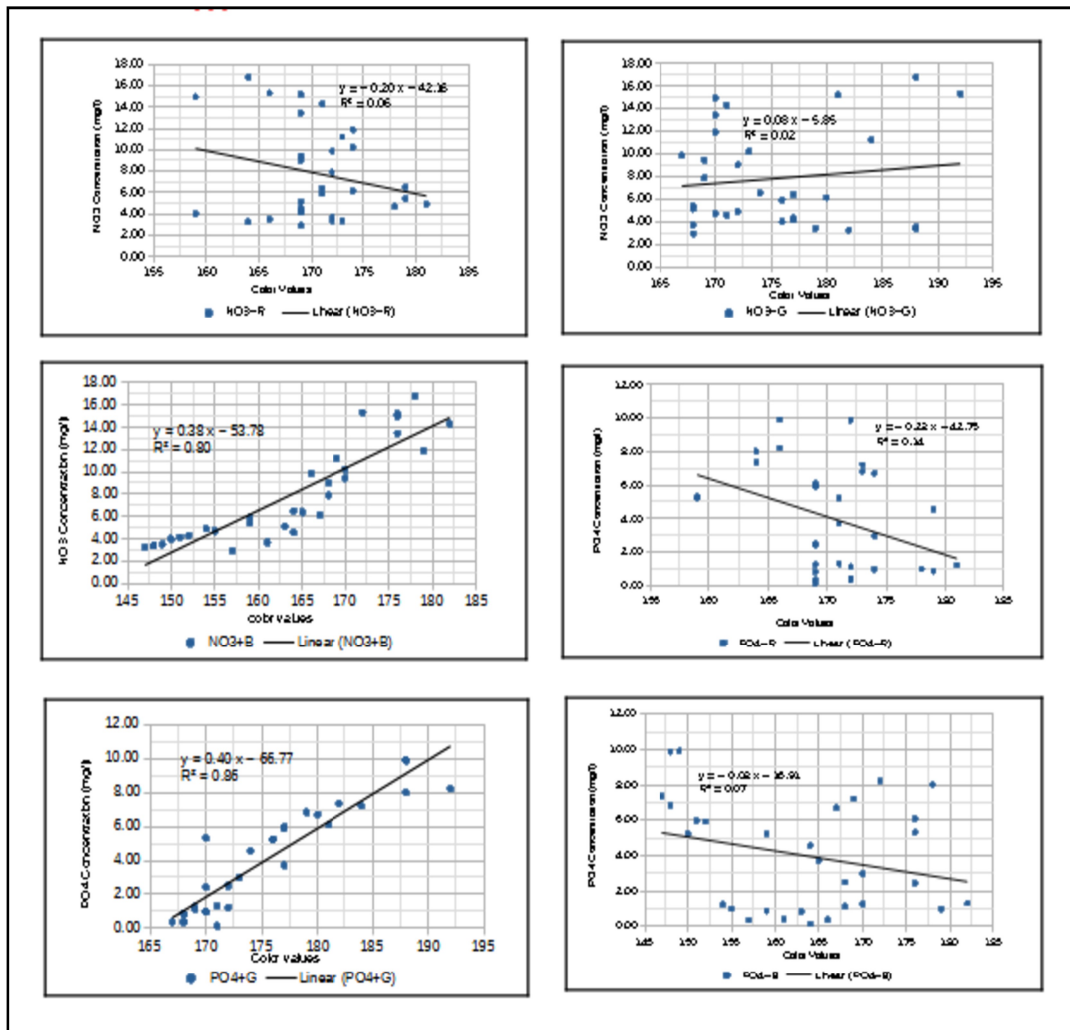


Figure 18. Power Relation between Nitrate, Phosphate Concentrations and Nix QC Sensor RGB Values

As discussed above, it is also important to validate the correlation between variable concentration and color results using a model function. A validation model was calculated for the nitrate parameter and relevant blue color data. As shown in figure 19., the validation model was computed using the following equation: $y = 0.38x - 53.78$. Therefore, in this linear regression model, NO₃ concentration and blue color results, according to the above equation, were fitted together with high accuracy.

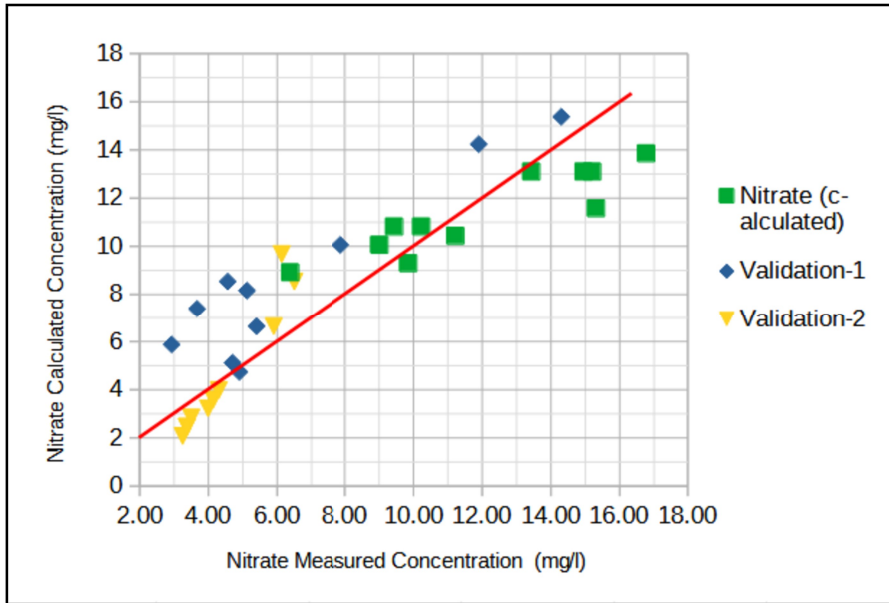


Figure 2. Nitrate Concentration and Nix QC Blue Color Validation Model.

The linear relationship between phosphate and the green channel is shown in Figure 20. A function was fitted to the data that provided an equation for adjusting the level of phosphate concentration and the green color. When applying this equation ($y = 0.40x - 66.77$). Compared to other methods for measuring phosphate, this accuracy is more than sufficient to collect meaningful phosphate measurements in inland waters.

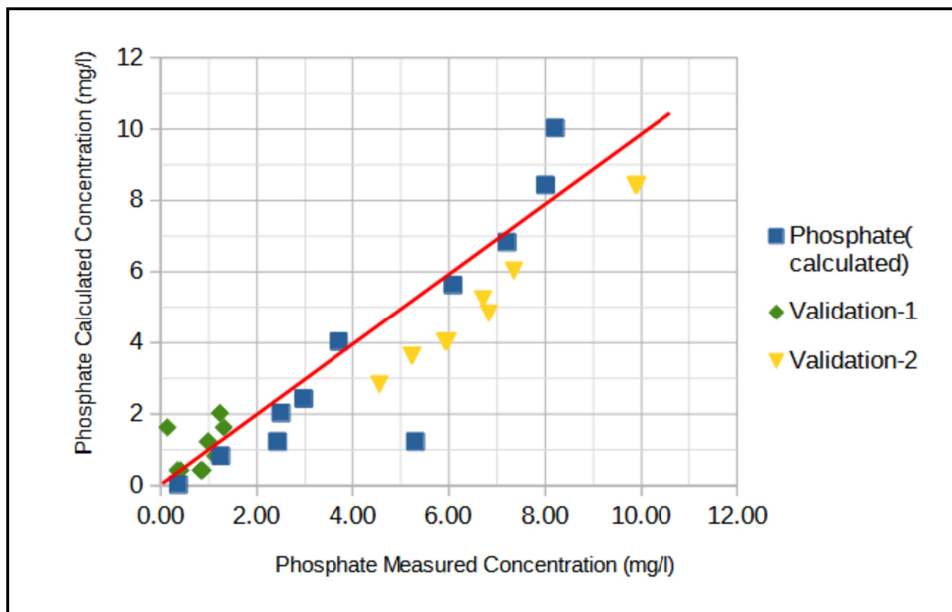


Figure 20. Phosphate Concentration and Nix QC Green Color Validation Model.

4.3 Smartphone camera image analysis

Estimating the quality of water using a smartphone camera became accessible to measure the color of the water. The red, green, and blue (RGB) color result that were acquired from the image were detected by the smartphone camera. Hence, the red, green, and blue (RGB) color values of the image were analysed to estimate the water quality of the reservoir using a cellphone application.

Statistical analyses were computed for the RGB color value. The minimum and maximum color values that were obtained from the colormeter cellphone application were 117 and 179 for blue and green, respectively. The highest standard deviation was obtained from Blue (16.15), and the lowest result was determined from Red (7.97). Moreover, the statistical variation computed from the three RGB color results was very small, less than 20 (Table 3.). The green part of the color shows a high average result (163), while the red part shows a lower average result (138).

Table 3. Statistical Analysis Smartphone RGB Color Results.

| Statistics | Smartphone Color Values | | |
|--------------------|-------------------------|------|-------|
| | R | G | B |
| Color values | | | |
| Minimum | 120 | 151 | 117 |
| Maximum | 158 | 179 | 175 |
| Mean | 138 | 163 | 143 |
| Standard Deviation | 7.97 | 9.03 | 16.15 |
| % CV | 5.76 | 5.54 | 11.15 |
| Correlation (PO4) | 0.08 | 0.99 | 0.03 |
| Correlation (NO3) | 0.19 | 0.08 | 0.96 |

The RGB color results obtained from the water reservoir to estimate water quality displayed in Figure 21. The green was dominant over red and blue colors. Thus, the highest peak was recorded from green and the lowest recorded from blue.

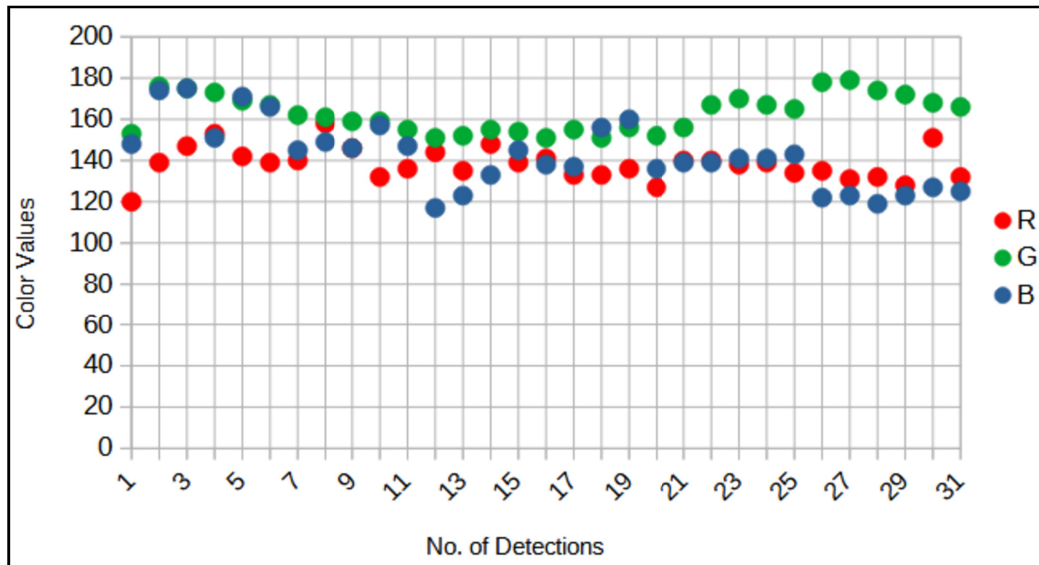


Figure 21. Smartphone Camera RGB Color Values Scatter Graph.

The amounts of nitrate and phosphate measured by the eXact iDip photometer were typically correlated with the colors red, green, and blue (RGB) of the pond waters. Assessments of the water variables and color data were analysed statistically. The nitrate parameter is substantially connected with blue, while the phosphate variable is connected with green (G), while both parameters are not significantly correlated with the red (R) color channel (Table 3.). The photometer findings for nitrate and phosphate concentration indicate a strong relationship between blue and green, respectively. whereas as the red channel were inversely correlated with nitrate and phosphate concentration

Figure 22 shows the findings of a linear regression correlation coefficient between the concentrations of nitrate and phosphate and RGB values obtained from smartphone camera. Nitrate concentrations show a strong positive linear relationship with blue (NO₃/B), and its regression coefficient was $R^2 = 0.92$, but a weak positive linear relationship was obtained from red and green with $R^2 = 0.04$ and $R^2 = 0.01$ consecutively. However, phosphate concentration with green (PO₄/G) shows a positive linear relationship with $R^2 = 0.98$ while the red and blue color results showed a weak linear relationship with $R^2 = 0.01$ and $R^2 = 0.00$ accordingly.

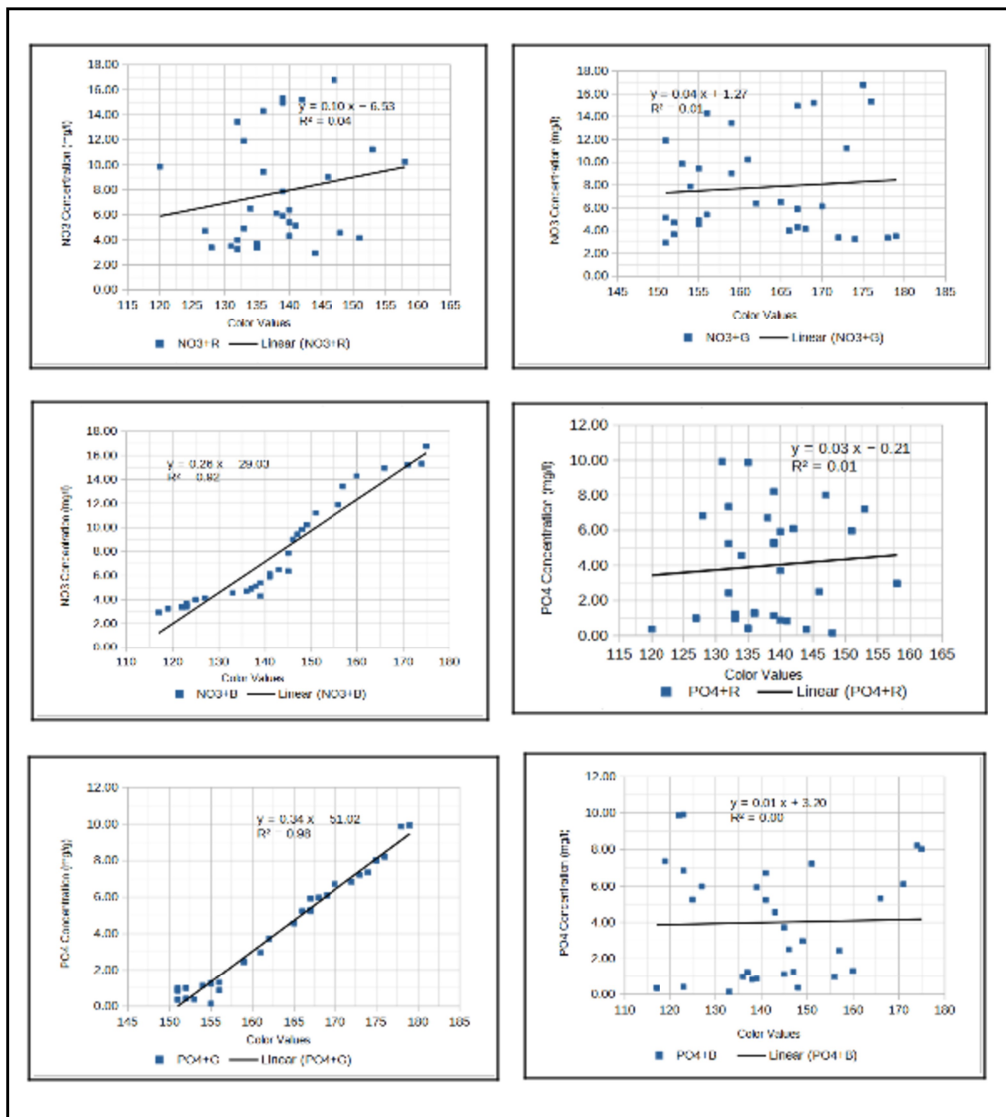


Figure 22. Power Relation between Nitrate, Phosphate Concentrations and Smartphone Camera RGB Color Values.

The appropriate cellphone blue color data and the nitrate parameter were used to create a validation model. The validation model was calculated using the equation $y = 0.26x - 29.03$, as illustrated in figure 23. As a result, the NO₃ concentration and blue color findings from the preceding equation were accurately fitted together in this linear regression model.

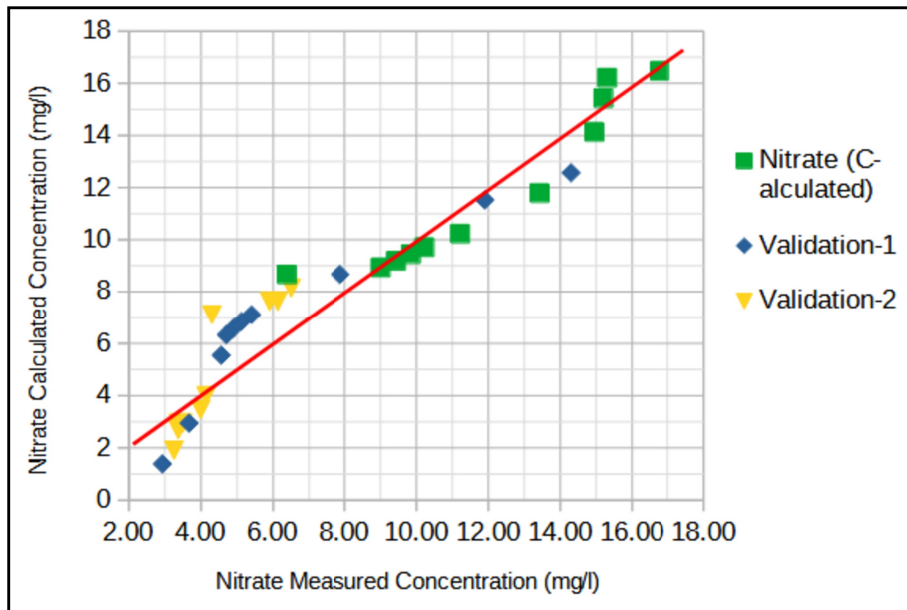


Figure 23. Nitrate Concentration and Smartphone Blue Color Validation Model.

Figure 24., depicts a linear connection between phosphate and the green channel. An equation for modifying the level of phosphate content and the green hue was produced by fitting a function to the data. When using the formula $y = 0.34x - 51.02$. This accuracy is well than enough to gather useful phosphate information of the water quality.

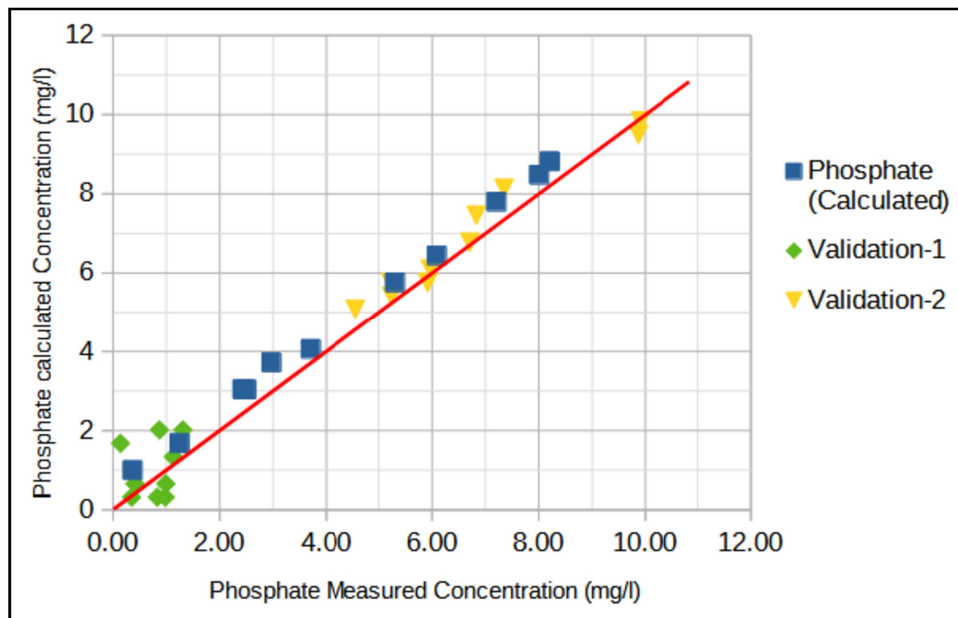


Figure 24. Phosphate Concentration and Smartphone Green Color Validation Model.

4.4 Nix QC and Smartphone Results Comparison

Comparing and contrasting Nix QC and Smartphone was about identifying both similarities and differences between these two methods using CIELAB color model. The CIELAB is currently used and recommended, because it uniformly covers the full visible spectrum of the human eye.

The color CIELAB values obtained from Nix QC was lighter than the brightness of CIELAB values obtained from smartphone camera with an average brightness of 71% and 65% accordingly. There was no significant difference between NIX QC and smartphone brightness. Color CIELab quality patterns indicate that as heterogeneity increase the water become darker in color. The colour parameters related to the CIELAB lightness or brightness are summarized in Figure 25.

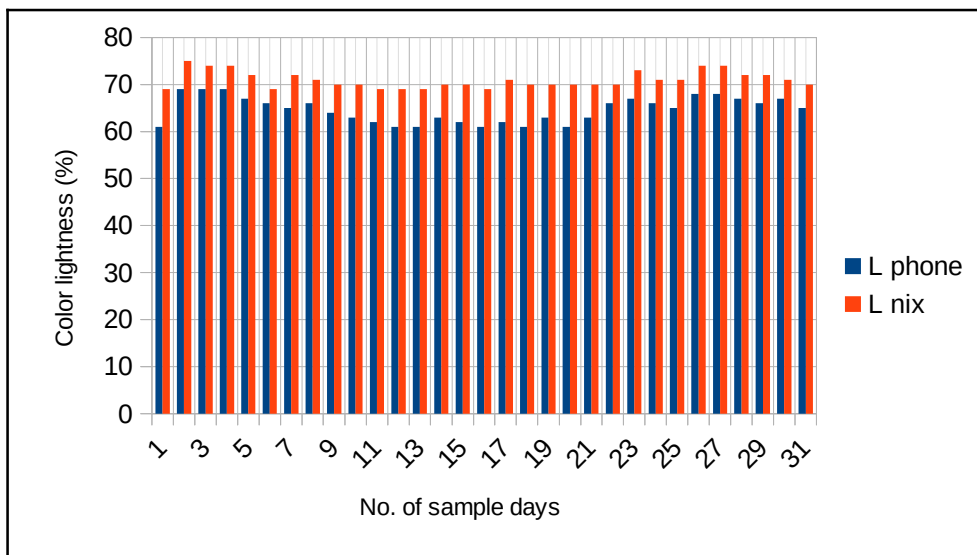


Figure 25. Nix QC and Smartphone CIELAB Lightness Comparison Graph.

A scatter plot is the most useful display technique for comparing two qualitative variables. We plot on the y-axis the variable we consider the response variable, and on the x-axis we place the predictor variable. In the CIELAB system, the a^* coordinate has negative values for greenish colors and positive values for reddish colors. The b^* coordinate has positive values for yellowish colors and negative values for blueish colors. The similarity and differences for a^*b^* of the CIELAB sphere are illustrated in Figure 26. We noticed that the water reservoir looked more bluish as cellphone cameras were made from the pond sides towards the clearer

waters in the middle, while the sides looked greenish. The probability of the green color of the sides of the reservoir is due to nitrate and phosphate concentrations entering from the surrounding environment. This was confirmed from the digital analysis of the pictures taken by CIELAB from the water reservoir (Figure 26.). The scatter plot showed a decreasing response in the red channel (R) with a corresponding increased response in the green channel (G) and, to a lesser extent, in the blue channel (B) in both Nix color sensor and smartphone techniques.

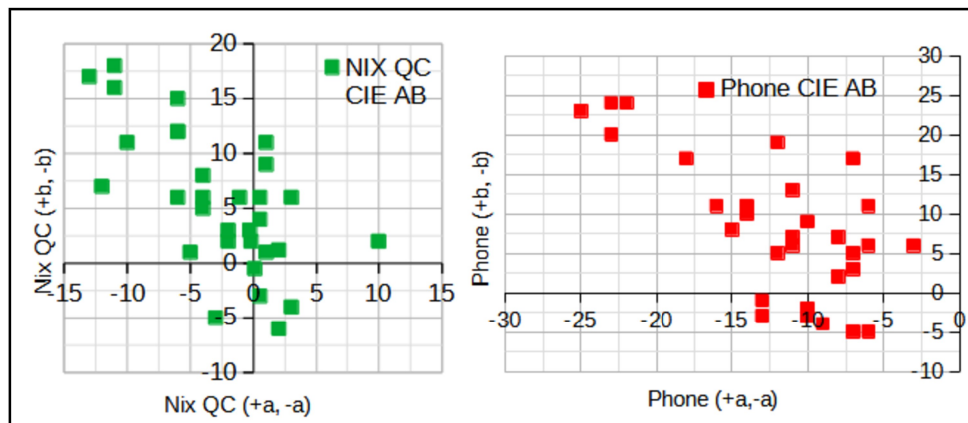


Figure 26. CIELAB Lightness Scatter Plot between Nix QC and Smartphone.

The camera's CIELAB lightness values should correlate with the standard color sensor. For this data set, simple correlations have indicated no improvement in the regressions to the water quality parameters using CIELAB differences. These facts, together with the fact that we wanted to compare camera results with Nix Quality Control methods using standard forms for the relationships, determined the use of color ratios rather than differences, with a lower proportion of bright blue and higher proportion of green color. Color saturation decreased with increasing water clarity. A highly significant linear correlation ($R^2 = 0.71$)

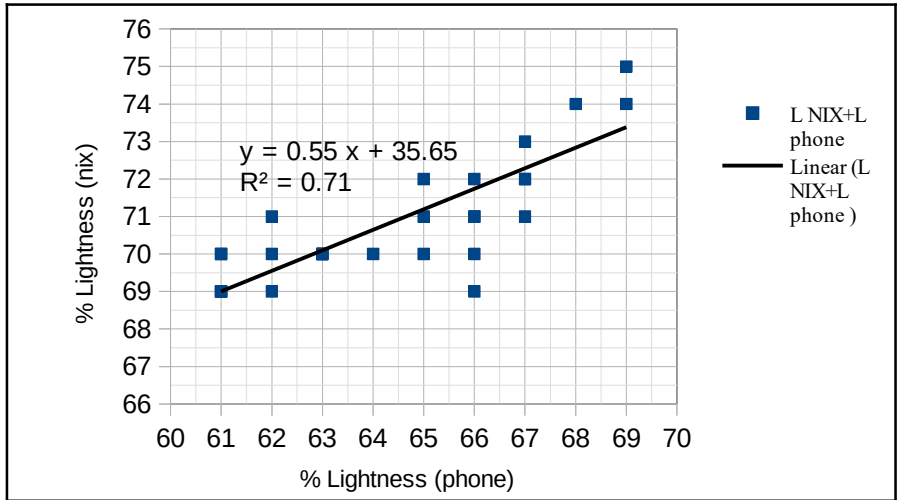


Figure 27. Correlation between Nix QC and Smartphone Camera CIELAB Results.

A validation model was constructed to compare and contrast Nix Quality Control results with smartphone results to estimate the accuracy of smartphones in field image data collection and also to predict water variables of waterbodies using the lightness (L) portion of the CIELAB system. As shown in Figure 27., the validation model was computed using the equation $y = 0.55x - 35.65$. This linear regression model successfully fitted for the lightness of both the Nix color sensor and the smartphone camera (Figure 28.).

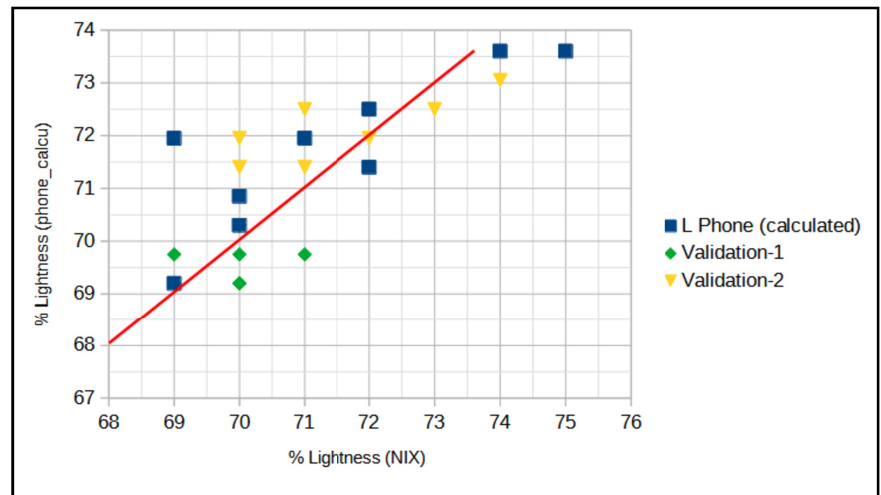


Figure 28. Nix QC and Smartphone regression model analysis.

5. CONCLUSION AND RECOMMENDATION

The primary goal of this study was to strengthen the monitoring, evaluation, and governance of surface water quality and to find out how communities react to smartphone water quality assessment applications in terms of their efficaciousness, usefulness, and contentment compared to analytical instruments. Besides, this work focuses on digital pictures on smartphones for the investigation of water quality, including the fundamentals of the technology, the tools used to capture images, the color spaces used, and the handling of research analysis.

Analytical water quality monitoring mainly relies on collecting water samples on site and sending them to the laboratory to measure various water quality parameters. This Analytical has the advantage that many different water quality parameters can be measured; Analytical techniques in laboratory practice are characterized by high precision, accuracy, sensitivity, and selectivity. However, the disadvantage is that water quality data can only be collected at limited time points, and the sampling interval is usually long. This is because such sampling usually requires professional equipment and trained technicians, and many of the instruments are expensive, heavy, inconvenient to carry, and labor intensive.

It is nearly hard to get temporal as well as spatial fluctuations of quality indicators for huge waterbodies using in-situ data collectors, which can only reflect point estimations of the general state of water circumstances in time and space. Water quality variable measurements and in-situ sampling require a lot of time, effort, and money. It is nearly impossible to investigate the geographical and temporal fluctuations and health of the water in vast waterbodies. The topography, for instance, may make monitoring, forecasting, and management of entire waterbodies impossible.

Mobility and growing acceptance of smartphones, the widespread usage of digital photos, and the enhanced development of cellphone APPs, there are currently chances to create on-the-spot, quick, affordable, and qualitative studies of water quality. Smartphone and hand held digital camera usage is significantly more prevalent than that of webcams and scanners thanks to their portability and light weight. Because of their rapid adoption, impressive advancements in camera capabilities, and extensive use of mobile applications, cellphones are

more frequently employed than digital cameras as image acquisition equipment for color measurement.

Image analysis has become a popular research issue in contemporary life. Smartphone image processing has advanced significantly thanks to its widespread use, powerful computing power, accessibility to everyone, and clear trend for varied measures, interpretation, and online sharing of data among manufacturers, customers, and governments. The photographic elements of the smartphone's cameras are of higher quality as the device gets newer.

This study established that there exists a statistically significant correlation between the phosphate water quality variable and green remote sensing. Besides, there was a strong correlation between nitrate and blue. With an appropriate method of linear regression algorithms, the retrieval of the NO_3 and PO_4 content was validated. These accuracy levels were acceptable for the practical application of routine monitoring and early warning for water quality safety with the support of precise traditional monitoring.

With advances in space science and the increasing use of computer applications and increased computing powers over recent decades, remote sensing techniques have become useful tools to achieve this goal. Remote sensing techniques make it possible to monitor and identify large scale regions and waterbodies that suffer from qualitative problems in a more effective and efficient manner. The collection of remotely sensed data occurs in digital form and therefore is easily readable in computer processing.

More research is needed to study the digital camera's response under different light circumstances and its possibility to provide absolute colour information. Until then a calibration with ground truth samples are necessary. When a calibration is not available, digital pictures can still be used to measure relative differences in colour from one region to another. In the future, Color Analysis smartphone application should be linked to an online database where users can upload their measurements, thus crowdsourcing water quality data.

6. SUMMARY

ANALYSIS OF SURFACE WATER WITH SPECTRAL PROPERTIES OF LIGHT

Author: Kiflu Hiyabu Jimie

Course, level of education: Environmental Engineering Master Science

Host Department/Institute: Institute of Environmental Sciences

Primary Supervisor: Dr. András Barczy, Assistant Professor, Institute of Environmental Sciences.

Text formatting: Times New Roman, 12 point size, 1,5 spacing, both side justified, top and bottom margins – 2.5 cm, right and left side margins 2,5 cm.

The goal of the current study is to investigate the feasibility of estimating water composition from the optical characteristics of the water surface using a conventional digital camera as a low-cost alternative method and to find out how communities react to smartphone water quality assessment applications in terms of their efficacy, usefulness, and contentment compared to conventional instruments. The advanced computing power and feasibility of use in various applications make smartphones a potential tool for surfacewater quality monitoring. In winter 2022/2023, field measurements were carried out on number Four fish Pond, Gödöllő-Állami telepek, Hungary. The absolute or relative reflectance between channels can be used to estimate both nitrate and phosphate substances detected with the Nix Quality Control (NIX QC) color sensor and smartphone camera method. In addition, a series of three-band pictures had been taken using a smartphone digital camera, and according to the results of the color analyser mobile application, the red, green, and blue bands of the water-leaving reflectance were calculated from these pictures. On this basis, the water nitrate and phosphate parameters were successfully estimated by comparing the calculated values of the color results obtained from the NIX QC and Smartphone with the analytical results obtained from the eXact iDip photometer. This study established that there exists a statistically significant correlation between the phosphate water quality variable and the green channel (PO_4/G). Besides, there was a strong power relation between nitrate and blue channel (NO_3/B). With an appropriate method of linear regression algorithms, the retrieval of the NO_3 and PO_4 content was validated. With the help of accurate traditional monitoring, this degree of accuracy was suitable for the practical implementation of regular assessment and early alarming for the security of the surface water.

7. ACKNOWLEDGEMENT

First and foremost, praises and thanks to the God the almighty, for his showers of blessings throughout my research work to complete the research successfully.

Firstly, I would like to express my deep and sincere gratitude to my research supervisor, Dr. Andras Bracz, for giving me the opportunity to do research and providing invaluable steadfast guidance throughout the gestation, writing, and editing of my thesis, despite frequently (and certainly understandably) having no idea what I was attempting to articulate. Completing this thesis would have been much more difficult without the enthusiasm and encouragement I received from him, both to celebrate progress and to console setbacks. His dynamism, vision, sincerity and motivation have deeply inspired me. I would also like to thank him for his friendship and Empathy.

My gratitude extends Institute of Environmental Sciences, Hungarian University of Agriculture and Life Science who generously provided knowledge and expertise to my studies. Additionally, I would like to express gratitude to Dr. Gábor Géczi, Department of Environmental Technology Group for his treasured support. Words cannot express my gratitude to my professors committee for their invaluable patience and feedback.

I would not be in this country, nor would I be working towards this level of education if it was not for the support, both financially and emotionally. I am thankful for the government of Eritrea and Hungary, especially the Stipendium Hungaricum that has provided financial support for which this thesis grew.

I am extremely grateful to my parent for their love, prayers, caring and sacrifices for educating and preparing me for my future. I am very much thankful to my wife and my daughters for their love, understanding, prayers and continuing support to complete this research work. Also I express my thanks to my brothers and sisters for their support and valuable prayers.

Thank you
Kiflu Hiyabu Jimie

8. REFERENCES

- Abdelmalik, K. W. (2018). Role of statistical remote sensing for Inland water quality parameters prediction. *Egyptian Journal of Remote Sensing and Space Science*, 21(2), 193–200. <https://doi.org/10.1016/j.ejrs.2016.12.002>
- Abughrin, S., Alshana, U., & Caleb, J. (2022). Smartphone Digital Image Colorimetry for the Determination of Aluminum in Antiperspirant Products. *Turkish Journal of Pharmaceutical Sciences*, 19(6), 618–625. <https://doi.org/10.4274/tjps.galenos.2021.18828>
- Acta, A. C., & Muri, J. (1962). A modified single solution method for the determination of phosphate in natural waters. *Analytica Chimica Acta*, 27, 31–36.
- Al-shaibah, B., Liu, X., Zhang, J., Tong, Z., & Zhang, M. (2021). Modeling Water Quality Parameters Using Landsat Multispectral Images : A Case Study of Erlong Lake ., *Remote Sensing*, 13, 1603.
- Alves, E. M., Rodrigues, R. J., dos Santos Corrêa, C., Fidemann, T., Rocha, J. C., Buzzo, J. L. L., de Oliva Neto, P., & Núñez, E. G. F. (2018). Use of ultraviolet–visible spectrophotometry associated with artificial neural networks as an alternative for determining the water quality index. *Environmental Monitoring and Assessment*, 190(6), 319. <https://doi.org/10.1007/s10661-018-6702-7>
- Bansod, B., Singh, R., & Thakur, R. (2018). Analysis of water quality parameters by hyperspectral imaging in Ganges River. *Spatial Information Research*, 26(2), 203–211. <https://doi.org/10.1007/s41324-018-0164-4>
- Bhateria, R., & Jain, D. (2016). Water quality assessment of lake water: a review. *Sustainable Water Resources Management*, 2, 161–173. <https://doi.org/10.1007/s40899-015-0014-7>
- Bhatti, U. A., Ming-Quan, Z., Huo, Q., Ali, S., Hussain, A., Yuhuan, Y., Yu, Z., Yuan, L., & Nawaz, S. A. (2021). Advanced Color Edge Detection Using Clifford Algebra in Satellite Images. *IEEE Photonics Journal*, 13(2), 1–20. <https://doi.org/10.1109/JPHOT.2021.3059703>
- Blaise, P., & Pétry, P. (1968). The Luminous Intensity and Range of Lights. *Journal of Navigation*, 21(3), 285–296. <https://doi.org/10.1017/S0373463300024759>
- Bokingkito, P. B., & Caparida, L. T. (2021). Usability evaluation of a real-time water quality monitoring mobile application. *Procedia Computer Science*, 197, 642–649. <https://doi.org/10.1016/j.procs.2021.12.185>
- Cantrell, K., Erenas, M. M., De Orbe-Payá, I., & Capitán-Vallvey, L. F. (2010). Use of the hue parameter of the hue, saturation, value color space as a quantitative analytical parameter

- for bitonal optical sensors. *Analytical Chemistry*, 82(2), 531–542.
<https://doi.org/10.1021/ac901753c>
- Cao, M., Hu, A., Gad, M., Adyari, B., Qin, D., Zhang, L., Sun, Q., & Yu, C. P. (2022). Domestic wastewater causes nitrate pollution in an agricultural watershed, China. *Science of the Total Environment*, 823, 153680.
<https://doi.org/10.1016/j.scitotenv.2022.153680>
- Carolina, N. (2002). Harmful Algal Blooms and Eutrophication Nutrient Sources , Composition , and Consequences. *Estuaries*, 25(4), 704–726.
- Chaplin, M. F. (2001). Water: Its importance to life. *Biochemistry and Molecular Biology Education*, 29(2), 54–59. [https://doi.org/10.1016/S1470-8175\(01\)00017-0](https://doi.org/10.1016/S1470-8175(01)00017-0)
- Clydesdale, F. M., & Ahmed, E. M. (1978). Colorimetry — methodology and applications. *Critical Reviews in Food Science and Nutrition*, 10(3), 243–301.
- Correll, D. L. (1998). The Role of Phosphorus in the Eutrophication of Receiving Waters: A Review. *Journal of Environmental Quality*, 27(2), 261–266.
<https://doi.org/10.2134/jeq1998.00472425002700020004x>
- Crowell, B. (2000). *Optics*. Light and Matter.
- Das, P., Chetry, B., Paul, S., Sundar, S., & Nath, P. (2022). Detection and quantification of phosphate in water and soil using a smartphone. *Microchemical Journal*, 172, 106949.
<https://doi.org/10.1016/j.microc.2021.106949>
- Eickhout, B., Bouwman, A. F., & van Zeijts, H. (2006). The role of nitrogen in world food production and environmental sustainability. *Agriculture, Ecosystems and Environment*, 116(1–2), 4–14. <https://doi.org/10.1016/j.agee.2006.03.009>
- Fan, Y., Li, J., Guo, Y., Xie, L., & Zhang, G. (2021). Digital image colorimetry on smartphone for chemical analysis: A review. *Measurement: Journal of the International Measurement Confederation*, 171, 108829.
<https://doi.org/10.1016/j.measurement.2020.108829>
- Gao, M., Li, J., Wang, S., Zhang, F., Yan, K., Yin, Z., & Xie, Y. (2022). Smartphone – Camera – Based Water Reflectance Measurement and Typical Water Quality Parameter Inversion. *Remote Sensing*, 14(6), 1371.
- Gardi, L. (2018). Planck ’ s Constant and the Nature of Light. *ResearchGate*.
<https://doi.org/10.13140/RG.2.2.29763.09767>
- Gholizadeh, M. H., Melesse, A. M., & Reddi, L. (2016). A comprehensive review on water quality parameters estimation using remote sensing techniques. *Sensors (Switzerland)*, 16(8). <https://doi.org/10.3390/s16081298>

- Goddijn-murphy, L., Dailloux, D., White, M., & Bowers, D. (2009). Fundamentals of in Situ Digital Camera Methodology for Water Quality Monitoring of Coast and Ocean. *Sensors*, *9*, 5825–5843. <https://doi.org/10.3390/s90705825>
- Goddijn, L. M., & White, M. (2006). Using a digital camera for water quality measurements in Galway Bay. *Estuarine, Coastal and Shelf Science*, *66*, 429–436. <https://doi.org/10.1016/j.ecss.2005.10.002>
- Guo, Y., Liu, C., Ye, R., & Duan, Q. (2020). Advances on water quality detection by uv-vis spectroscopy. *Applied Sciences (Switzerland)*, *10*(19), 6874. <https://doi.org/10.3390/app10196874>
- Hamilton, D. P., Salmaso, N., & Paerl, H. W. (2016). Mitigating harmful cyanobacterial blooms : strategies for control of nitrogen and phosphorus loads. *Aquatic Ecology*, *50*(3), 351–366. <https://doi.org/10.1007/s10452-016-9594-z>
- He, W., Chen, S., Liu, X., & Chen, J. (2008). Water quality monitoring in a slightly-polluted inland water body through remote sensing - Case study of the Guanting Reservoir in Beijing, China. *Frontiers of Environmental Science and Engineering in China*, *2*(2), 163–171. <https://doi.org/10.1007/s11783-008-0027-7>
- Heidari-Bafroui, H., Charbaji, A., Anagnostopoulos, C., & Faghri, M. (2021). A colorimetric dip strip assay for detection of low concentrations of phosphate in seawater. *Sensors*, *21*(9), 3125. <https://doi.org/10.3390/s21093125>
- Hoang, M. A., ã, J. G., & Smeulders, A. W. M. (2005). Color texture measurement and segmentation. *Signal Processing*, *85*(2), 265–275. <https://doi.org/10.1016/j.sigpro.2004.10.009>
- Huang, C., Shi, K., Yang, H., Li, Y., Zhu, A. X., Sun, D., Xu, L., Zou, J., & Chen, X. (2015). Satellite observation of hourly dynamic characteristics of algae with Geostationary Ocean Color Imager (GOCI) data in Lake Taihu. *Remote Sensing of Environment*, *159*, 278–287. <https://doi.org/10.1016/j.rse.2014.12.016>
- Isgro, M. A., Basallote, M. D., Caballero, I., & Barbero, L. (2022). Comparison of UAS and Sentinel-2 Multispectral Imagery for Water Quality Monitoring: A Case Study for Acid Mine Drainage Affected Areas (SW Spain). *Remote Sensing*, *14*(16). <https://doi.org/10.3390/rs14164053>
- Jiang, J., Tang, S., Han, D., Fu, G., Solomatine, D., & Zheng, Y. (2020). A comprehensive review on the design and optimization of surface water quality monitoring networks. *Environmental Modelling and Software*, *132*, 104792. <https://doi.org/10.1016/j.envsoft.2020.104792>

- Juncal, M. J. L., Skinner, T., Bertone, E., & Stewart, R. A. (2020). Development of a real-time, mobile nitrate monitoring station for high-frequency data collection. *Sustainability*, *12*(14), 5780. <https://doi.org/10.3390/su12145780>
- Karpatne, A., Khandelwal, A., Chen, X., Mithal, V., Faghmous, J., & Kumar, V. (2016). Global monitoring of inland water dynamics: State-of-the-art, challenges, and opportunities. *Studies in Computational Intelligence*, *645*, 121–147. https://doi.org/10.1007/978-3-319-31858-5_7
- Khattab, M. F. O., & Merkel, B. J. (2014). Application of Landsat 5 and Landsat 7 images data for water quality mapping in Mosul Dam Lake , Northern Iraq Image Enhancement via Lookup Table. *Arabian Journal of Geosciences*, *7*, 3557–3573. <https://doi.org/10.1007/s12517-013-1026-y>
- Kröckel, L., Lehmann, H., Wieduwilt, T., & Schmidt, M. A. (2014). Talanta Fluorescence detection for phosphate monitoring using reverse injection analysis. *Talanta*, *125*, 107–113. <https://doi.org/10.1016/j.talanta.2014.02.072>
- Kuehni, R. G. (2001). Color space and its divisions. *Color Research and Application*, *26*(3), 209–222. <https://doi.org/10.1002/col.1018>
- Lazur, A. M., Cichra, C. E., & Watson, C. (2013). The Use of Lime in Fish Ponds. *University of Florida Cooperative Extension Service, Institute of Food and Agriculture Sciences, Southern Regional Aquaculture Center*, 4606, 1–3.
- Leeuw, T., & Boss, E. (2018). The HydroColor App : Above Water Measurements of Remote Sensing Reflectance and Turbidity Using a Smartphone Camera. *Sensors (Switzerland)*, *18*(1), 256. <https://doi.org/10.3390/s18010256>
- Liu, F. S., Lockett, B. R., Sorichetti, R. J., Watmough, S. A., & Eimers, M. C. (2022). Agricultural intensification leads to higher nitrate levels in Lake Ontario tributaries. *Science of the Total Environment*, *830*, 154534. <https://doi.org/10.1016/j.scitotenv.2022.154534>
- Maloney, L. T., & Brainard, D. H. (2010). Color and material perception : Achievements and challenges Surface material perception : *Vission*, *10*(9), 1–6. <https://doi.org/10.1167/10.9.19.Introduction>
- Malthus, T. J., Ohmsen, R., & van der Woerd, H. J. (2020). An evaluation of citizen science smartphone apps for Inland water quality assessment. *Remote Sensing*, *12*(10). <https://doi.org/10.3390/rs12101578>
- Mar, S. U., & Qbal, M. I. (2007). Review article Nitrate accumulation in plants , factors affecting the process , and human health implications . A review. *Agronomy Sustainable Development*, *27*, 45–57. <https://doi.org/10.1051/agro>

- Ménesguen, A., Desmit, X., Dulière, V., Lacroix, G., Thouvenin, B., Thieu, V., & Dussauze, M. (2018). How to avoid eutrophication in coastal seas ? A new approach to derive river-specific combined nitrate and phosphate maximum concentrations. *Science of the Total Environment*, *628*, 400–414. <https://doi.org/10.1016/j.scitotenv.2018.02.025>
- Mironov, N., Haque, M., Atfi, A., & Razzaque, M. S. (2022). Phosphate Dysregulation and Metabolic Syndrome. *Nutrients*, *14*(21), 4477. <https://doi.org/10.3390/nu14214477>
- Mng'ong'o, M. E., Munishi, L. K., & Ndakidemi, P. A. (2022). Increasing agricultural soil phosphate (P) status influences water P levels in paddy farming areas : Their implication on environmental quality. *Case Studies in Chemical and Environmental Engineering*, *6*, 100259. <https://doi.org/10.1016/j.cscee.2022.100259>
- Olmanson, L. G., Brezonik, P. L., & Bauer, M. E. (2013). Airborne hyperspectral remote sensing to assess spatial distribution of water quality characteristics in large rivers: The Mississippi River and its tributaries in Minnesota. *Remote Sensing of Environment*, *130*, 254–265. <https://doi.org/10.1016/j.rse.2012.11.023>
- Padilla-mendoza, C., Torres-bejarano, F., Campo-daza, G., & Carlos, L. (2023). Potential of Sentinel Images to Evaluate Physicochemical Parameters Concentrations in Water Bodies — Application in a Wetlands System in Northern Colombia. *Water*, *15*, 789.
- Peng, J., Jin, C., Wu, Y., Hou, Z., Gao, S., & Chu, Z. (2022). Modeling Non-Point Source Nutrient Loads with Different Cropping Systems in an Agricultural Lake Watershed in Southwestern China : From Field to Watershed Scale. *Mathematics*, *10*(21), 4047.
- Phuangsaikai, N., Jakmunee, J., & Kittiwachana, S. (2021). Investigation into the predictive performance of colorimetric sensor strips using RGB, CMYK, HSV, and CIELAB coupled with various data preprocessing methods: a case study on an analysis of water quality parameters. *Journal of Analytical Science and Technology*, *12*(1), 1–16. <https://doi.org/10.1186/s40543-021-00271-9>
- Pires, N. M. M., Dong, T., Hanke, U., & Hoivik, N. (2014). Recent developments in optical detection technologies in lab-on-a-chip devices for biosensing applications. *Sensors (Switzerland)*, *14*(8), 15458–15479. <https://doi.org/10.3390/s140815458>
- Qin, B. (2009). Lake eutrophication: Control countermeasures and recycling exploitation. *Ecological Engineering*, *35*(11), 1569–1573. <https://doi.org/10.1016/j.ecoleng.2009.04.003>
- Quemada, M., & Gabriel, J. L. (2016). Approaches for increasing nitrogen and water use efficiency simultaneously. *Global Food Security*, *9*, 29–35. <https://doi.org/10.1016/j.gfs.2016.05.004>
- Reddy, S. K. K., Gupta, H., Reddy, D. V., & Kumar, D. (2021). The suitability of surface waters from small west-flowing rivers for drinking, irrigation, and aquatic life from a

- global biodiversity hotspot (Western Ghats, India). *Environmental Science and Pollution Research*, 28(29), 38613–38628. <https://doi.org/10.1007/s11356-021-13154-8>
- Rout, P. R., Shahid, M. K., Dash, R. R., Bhunia, P., Liu, D., Varjani, S., Zhang, T. C., & Surampalli, R. Y. (2021). Nutrient removal from domestic wastewater: A comprehensive review on conventional and advanced technologies. *Journal of Environmental Management*, 296, 113246. <https://doi.org/10.1016/j.jenvman.2021.113246>
- Sajidu, S. M. I. (2007). *Water quality assessment in streams and wastewater treatment plants of Blantyre, Malawi*. 32, 1391–1398. <https://doi.org/10.1016/j.pce.2007.07.045>
- Sant'Anna, V., Gurak, P. D., Ferreira Marczak, L. D., & Tessaro, I. C. (2013). Tracking bioactive compounds with colour changes in foods - A review. *Dyes and Pigments*, 98(3), 601–608. <https://doi.org/10.1016/j.dyepig.2013.04.011>
- Schwarzenbach, R. P., Egli, T., Hofstetter, T. B., Von Gunten, U., & Wehrli, B. (2010). Global water pollution and human health. *Annual Review of Environment and Resources*, 35, 109–136. <https://doi.org/10.1146/annurev-environ-100809-125342>
- Shao-ting, D. U., Yong-song, Z., & Xian-yong, L. I. N. (2007). Accumulation of Nitrate in Vegetables and Its Possible Implications to Human Health. *Agricultural Sciences in China*, 6, 1246–1255.
- Song, K., Li, L., Li, S., Tedesco, L., Hall, B., & Li, L. (2012). Hyperspectral Remote Sensing of Total Phosphorus (TP) in Three Central Indiana Water Supply Reservoirs. *Water Air Soil Pollution*, 223, 1481–1502. <https://doi.org/10.1007/s11270-011-0959-6>
- Stone, N. M., & Thomforde, H. K. (2004). Understanding your fish pond water analysis report. *Cooperative Extension Program, University of Arkansas at Pine Bluff, US Department of Agriculture and County Governments*, 1–4. <http://www.ianrpubs.unl.edu/liveg.pdf>
- Swaney, D. P., Howarth, R. W., & Hong, B. (2018). Nitrogen use efficiency and crop production : Patterns of regional variation in the United States , 1987 – 2012. *Science of the Total Environment*, 635, 498–511. <https://doi.org/10.1016/j.scitotenv.2018.04.027>
- Thajee, K., Paengnakorn, P., Wongwilai, W., & Grudpan, K. (2018). Application of a webcam camera as a cost-effective sensor with image processing for dual electrochemical – colorimetric detection system. *Talanta*, 185(March), 160–165. <https://doi.org/10.1016/j.talanta.2018.03.055>
- Thiemann, S., & Kaufmann, H. (2000). Determination of Chlorophyll Content and Trophic State of Lakes Using Field Spectrometer and IRS-1C Satellite Data in the Mecklenburg Lake District, Germany. *Remote Sensing of Environment*, 235, 227–235.
- USEPA. (1994). *U.S. Environmental Protection Agency. 1994. Water quality standards handbook: second edition. EPA-823-B-94-005a.*

- Verhoeven, G. J. J. (2017). The reflection of two fields – Electromagnetic radiation and its role in (aerial) imaging. *AARGnews*, 55, 13–18. <https://doi.org/10.5281/zenodo.3534245>
- Verla, E. N., Verla, A. W., & Enyoh, C. E. (2020). Finding a relationship between physicochemical characteristics and ionic composition of River Nworie, Imo State, Nigeria. *PeerJ Analytical Chemistry*, 2, e5. <https://doi.org/10.7717/peerj-achem.5>
- Viscarra Rossel, R. A., Minasny, B., Roudier, P., & McBratney, A. B. (2006). Colour space models for soil science. *Geoderma*, 133(3–4), 320–337. <https://doi.org/10.1016/j.geoderma.2005.07.017>
- Wang, S., Li, J., Zhang, B., Spyrakos, E., Tyler, A. N., Shen, Q., Zhang, F., Kuster, T., Lehmann, M. K., Wu, Y., & Peng, D. (2018). Trophic state assessment of global inland waters using a MODIS-derived Forel-Ule index. *Remote Sensing of Environment*, 217(September), 444–460. <https://doi.org/10.1016/j.rse.2018.08.026>
- Ward, M. H., Id, R. R. J., Brender, J. D., Kok, T. M. De, Weyer, P. J., Nolan, B. T., Villanueva, C. M., & Breda, S. G. Van. (2018). Drinking Water Nitrate and Human Health : An Updated Review. *International Journal of Environmental Research and Public Health*, 15(7), 1557. <https://doi.org/10.3390/ijerph15071557>
- Web 1. (n.d.). Retrieved March 10, 2023, from <http://room7tp.blogspot.com/2017/03/the-electromagnetic-spectrum.html>
- web 2. (n.d.). Retrieved April 9, 2022, from <https://www.wateriga.com/products/exact-idip-smart-brew-starter-kit>
- Web 3. (n.d.). Retrieved January 13, 2023, from <https://www.itseurope.co.uk/collections/photometers/products/exact-idip-water-testing-photometer>
- WHO. (2008). *Guidelines for Drinking-water Quality. 1.*
- Wilkes, T. C., McGonigle, A. J. S., Pering, T. D., Taggart, A. J., White, B. S., Bryant, R. G., & Willmott, J. R. (2016). Ultraviolet imaging with low cost smartphone sensors: Development and application of a raspberry pi-based UV camera. *Sensors (Switzerland)*, 16(10), 1649. <https://doi.org/10.3390/s16101649>
- Xie, Y., Yu, X., Ng, N. C., Li, K., & Fang, L. (2018). Exploring the dynamic correlation of landscape composition and habitat fragmentation with surface water quality in the Shenzhen river and deep bay cross-border watershed, China. *Ecological Indicators*, 90, 231–246. <https://doi.org/10.1016/j.ecolind.2017.11.051>
- Xu, F., Leng, W., Lu, Q., Li, K., Zhang, Y., Liu, J., Xu, L., & Sheng, G. (2023). Ratiometric fluorescent sensing of phosphate ion in environmental water samples using flavin mononucleotide-functionalized Fe₃O₄ particles. *Science of the Total Environment*, 857, 159249. <https://doi.org/10.1016/j.scitotenv.2022.159249>

- Yalç, B., Artüz, M. L., Pavlidou, A., Çubuk, S., & Dassenakis, M. (2017). Nutrient dynamics and eutrophication in the Sea of Marmara : Data from recent oceanographic research. *Science of the Total Environment*, *602*, 405–424.
<https://doi.org/10.1016/j.scitotenv.2017.05.179>
- Yona, C., Makange, M., Moshiro, E., Chengula, A., & Misinzo, G. (2023). Water pollution at Lake Natron Ramsar site in Tanzania : A threat to aquatic life. *Ecohydrology & Hydrobiology*, *23*(1), 98–108. <https://doi.org/10.1016/j.ecohyd.2022.11.001>
- Zhang, H., Reardon, C., & Parker, L. E. (2013). Real-time multiple human perception with color-depth cameras on a mobile robot. *IEEE Transactions on Cybernetics*, *43*(5), 1429–1441. <https://doi.org/10.1109/TCYB.2013.2275291>
- Zhang, X., & Wandell, B. A. (1996). A spatial extension of CIELAB for digital color-image reproduction. *Society for Information Display*, *27*(1), 731–734.
<http://sci-hub.tw/http://onlinelibrary.wiley.com/doi/10.1889/1.1985127/pdf>
- Zhao, H. X., Liu, Q., Liu, Z. De, Wang, Y., & Zhao, J. (2011). ChemComm Highly selective detection of phosphate in very complicated matrixes with an off – on fluorescent probe of europium-adjusted carbon dots w. *Chemical Communication*, *47*(9), 2604–2606.
<https://doi.org/10.1039/c0cc04399k>

9. APPENDIX

Image Capturing Basic Guidelines

The three pillars of photography, such as; aperture, shutter speed and ISO certainly are the most important steps in photography.

Step 1. Aperture

Aperture can be defined as the opening in a lens through which light passes to enter the camera. It is an easy concept to understand if you just think about how your eyes work. As you move between bright and dark environments, the iris in your eyes either expands or shrinks, controlling the size of your pupil.

In photography, the “pupil” of your lens is called aperture. You can shrink or enlarge the size of the aperture to allow more or less light to reach your camera sensor.

Step 2. Shutter Speed

Once the light has passed through the aperture of the lens, it reaches the shutter. You need to decide how much of that light you’re going to allow into the camera. A very small fraction of a second (for example 1/250) will prevent motion. An even smaller fraction (for example 1/4000) for sports photography A really slow shutter speed (30 seconds) is perfect for night photography. It all depends on what you’re shooting and how much light you have available to you.

Step 3. ISO

Once the light has passed through the aperture and been filtered by the shutter speed, it reaches the sensor, where we decide upon the ISO. As you turn the ISO number up, you increase the exposure but, at the same time, the image quality decreases; there will be more digital noise or “grain”. So you have to decide upon your priorities in terms of exposure vs grain.

Color Conversion

Nix color quality control sensor color conversion from one model to another

Available in free color converter-RGB, CMYK, LAB, XYZ, HEX and more (nixsensor.com)

| Input | Output |
|---|---|
| L (0 to 100) <input type="text" value="0"/> | RGB (0 to 255): 0 0 0 |
| a (-128 to 128) <input type="text" value="0"/> | HEX (#): 000000 |
| b (-128 to 128) <input type="text" value="0"/> | CMYK (0% to 100%): 75% 68% 67% 90% |
| | CIELAB (0 to 100, -128 to 128, -128 to 128): 0.00 0.00 0.00 |
| | XYZ (0 to 0.9642, 0 to 1.0000, 0 to 0.8252): 0.0000 0.0000 0.0000 |
| | <input type="text"/> |

Settings

| | |
|--|-------------------------------------|
| Input system | <input type="text" value="CIELAB"/> |
| Illuminant and reference angle for input values | <input type="text" value="D50 2°"/> |
| Illuminant and reference angle for output values | <input type="text" value="D50 2°"/> |
| XYZ range 0 to 1 if checked | <input checked="" type="checkbox"/> |

Color picker; Calculator and generator with high precision and contrast test. Converts also RGB, HEX, HSV/HSB CMYK, CIELAB and others ([https:// colorizer.org](https://colorizer.org))

▼ **YPbPr (similar to YCbCr & YUV)**

Y 0.3

Pr -0.07

Pb -0.12

► Xyz

► xyY

▼ **Munsell (MHVC)** 8GY 3.7/7.7

Hue 37.66

Value 3.68

Chroma 7.68

▼ **Misc**

Alpha/Opacity 100

| | | |
|----------------------------------|--|--------------------------|
| ▼ RGB(A) | | rgb(50, 100, 20) |
| Red | | 50 |
| Green | | 100 |
| Blue | | 20 |
| Hex | | #326414 |
| ▼ HSL(A) | | hsl(97.5, 66.7%, 23.5%) |
| Hue | | 97.5 |
| Saturation | | 66.67 |
| Lightness | | 23.53 |
| ▶ HSV / HSB | | |
| ▼ CMYK | | cmyk(0.5, 0, 0.8, 0.608) |
| Cyan | | 50 |
| Magenta | | 0 |
| Yellow | | 80 |
| Key/Black | | 60.78 |
| ▼ Lab (CIELAB, CIE-L*a*b, L*a*b) | | lab(37.56, -31.78, 37.5) |
| Lightness | | 37.56 |
| A (Green→Red) | | -31.78 |
| B (Blue→Yellow) | | 37.5 |

10. DECLARATION

On Authenticity and Public Assess of Final Mater's Thesis

Student's name: **Kiflu Hiyabu Jimie**

Student's Neptun ID: **F78NTE**

Title of the document: **Analysis of Surfacewater with Spectral Properties of Light**

Year of publication: **May 2023**

Department: **Environmental Engineering**

I declare that the submitted final master's thesis is my own, original individual creation. Any parts taken from an another author's work are clearly marked, and listed in the table of contents.

If the statements above are not true, I acknowledge that the Final examination board excludes me from participation in the final exam, and I am only allowed to take final exam if I submit another final master's thesis.

Viewing and printing my submitted work in a PDF format is permitted. However, the modification of my submitted work shall not be permitted.

I acknowledge that the rules on Intellectual Property Management of Hungarian University of Agriculture and Life Sciences shall apply to my work as an intellectual property.

I acknowledge that the electric version of my work is uploaded to the repository sytem of the Hungarian University of Agriculture and Life Sciences.

Place and date: **Gödöllő, 2023** year **May** month **03** day



Student's signature

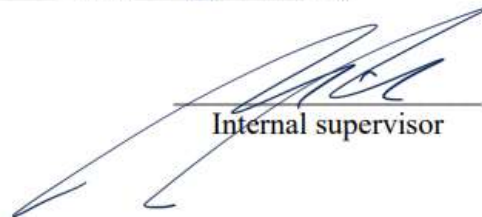
STATEMENT ON CONSULTATION PRACTICES

As a supervisor of **Kiflu Hiyabu Jimie** (Student's name) **F78NTE** (Student's NEPTUN ID), I here declare that the final essay/thesis/master's thesis/portfolio¹ has been reviewed by me, the student was informed about the requirements of literary sources management and its legal and ethical rules.

I recommend/don't recommend² the final essay/thesis/master's thesis/portfolio to be defended in a final exam.

The document contains state secrets or professional secrets: yes no^{*3}

Place and date: 2023 year 05. month 02. day


Internal supervisor